Light Propagation in a Warp Drive Spacetime

Michael Peter Kinach
Department of Physics
St. Francis Xavier University

March 27$^{\text{th}}$, 2017

Abstract

Within the context of general relativity, the Alcubierre metric (AM) provides a mathematical description of a "warp drive" spacetime that would allow an object to traverse a vast distance in an arbitrarily small time period. To an observer at rest in flat space, it looks as if the object has a speed $V > c$. This idea is analogous to the "warp drive" of science fiction and has led to the AM being coined the "Alcubierre warp drive". This thesis examines the propagation of electromagnetic waves in the two-dimensional AM. Conformal coordinate transformations are used to solve the electromagnetic wave equation. It is found that the apparent velocity of light will change as it passes through the boundary of a warp drive. It is also found that an electromagnetic wavepacket will undergo an apparent redshift or blueshift. For the case of a warp drive traveling at speeds faster than light, an apparent horizon forms. We conclude by analyzing this horizon using conformal light-cone coordinates.

Table of Contents

Appendices

List of Figures

Acknowledgments

I would like to acknowledge Dr. Karl-Peter Marzlin for invaluable assistance with this project. I would also like to recognize the faculty and staff of the Department of Physics at St. Francis Xavier University for their guidance and instruction. The Natural Sciences and Engineering Research Council of Canada graciously provided funding for the project. Finally, I want to thank my family and friends for their encouragement and support.

The textbook *Gravity* by J. B. Hartle [1] was referenced heavily for the mathematical overview presented in Section 1.3. The idea for the clever spring analogy presented in Section 1.1.1 comes from A. DeBenedictis [2]. Y. Fujii's *The Scalar-Tensor Theory of Gravitation* [3] was referenced for the overview of conformal transformations provided in Section 3.1. The textbook *A First Course in String Theory* by B. Zwiebach [4] was useful for writing the overview of light-cone coordinates in Chapter 4.

Chapter 1

Introduction

Gravity is one of the four fundamental interactions. Until the beginning of the twentieth century, Newton's *Law of Universal Gravitation* was the predominant mathematical model of gravity. This law states that two bodies of mass m_1 and m_2 will be pulled together by an attractive force given by

$$\vec{F} = -G\frac{m_1 m_2}{r^2}\hat{r} \tag{1.1}$$

where r is the distance between the bodies and G is the gravitational constant. Newton's simple model presumes that time and space are distinct and separate concepts. This assumption provides a fairly accurate description of the gravitational interaction for large objects moving at small velocities.

The introduction of Einstein's theory of special relativity in 1905 raised some serious doubts about Newton's basic assumption. Special relativity requires that the laws of physics must be identical for all non-accelerating observers. The theory also requires that the speed of light in a vacuum must be the same for all non-accelerating observers. These postulates are incompatible with the notion of time being conceptually distinct from space. Instead, space and time must be woven into a unified entity called *spacetime*.

Between 1905 and 1915, Einstein began developing a theory of gravity that was consistent with his new relativistic framework. This took the form of a geometric theory where gravity could be understood as curvature in spacetime. He proposed that mass and energy caused spacetime to curve in their vicinity and objects moved in straight lines according to this curvature. He called this theory *general relativity* because it was the generalization of his earlier theory of special relativity.

General relativity is one of the most successful theories in modern physics. Empirical measurements of the orbit of Mercury, the deflection of light by the Sun, and the gravitational redshift of light provided early support for general relativity in the decades after it was published [5] [6]. More recently, the detection of gravitational waves by the LIGO project [7] has reinforced the empirical evidence for the theory. Although many unanswered questions about general relativity still remain, its experimental success makes it one of the most widely studied theories of the gravitational interaction.

1.1 Warp Drive Spacetimes

In science fiction stories, a *warp drive* allows a spaceship to travel a vast cosmic distance in a short amount of time. This concept is convenient for stories where the setting is interstellar space and the backdrop spans millions of light-years. Unfortunately, the maximum possible speed that an object can reach is limited by the theory of special relativity. A massive object can never travel faster than c, the speed of light. It is also true that objects traveling at near-c speeds will experience *time dilation*, an effect where two observers in relative uniform motion will experience time elapsing at different rates. These limitations imply that faster-than-light travel is forbidden by special relativity.

Fortunately, special relativity isn't the whole story. It only describes regions where there is no mass or energy to generate curvature in spacetime. Within the context of general relativity, it has been proposed that certain mass-energy distributions could curve spacetime in a way that would permit apparent faster-than-light travel. This spacetime, commonly referred to as the *Alcubierre spacetime* or the *Alcubierre warp drive*, was first proposed by Miguel Alcubierre in 1994 [8].

1.1.1 Qualitative Description of a Warp Drive

The basic idea of the warp drive is to create a distortion of spacetime that corresponds to an expansion behind an object and a contraction in front of it. The result is that an object will be rapidly pulled forward and pushed from behind. In this manner it can circumvent the limitations of special relativity and make a trip to a distant galaxy in an arbitrarily short time.

To make this idea more tangible to the reader, I will use the analogy of a spring. At a basic level, spacetime can be thought of as a dynamical entity that can expand and contract. A spring can also expand and contract along one direction. Since they share this property, we can use an unstretched spring as a "toy model" of spacetime.

Suppose there is a galaxy at both ends of a spring of length L. A spaceship in the middle of the spring would have to travel a distance $L/2$ to reach one of the galaxies. If it traveled at the maximum possible speed that special relativity allows, it could take many thousands of years to reach its destination. However, in the Alcubierre warp drive, spacetime is distorted so that the region in front of the spaceship is compressed and the region behind it is expanded. In our toy model, this corresponds to the spring being stretched out behind the spaceship and compressed in front of it. This is illustrated in Fig. 1.1.

To an outside observer looking at the spring, it appears that the spaceship has moved much closer to the galaxy. Moreover, since there is no limitation to how quickly spacetime can compress and expand, it may appear the spaceship traveled at a speed V that is greater than c. Although this seems to violate special relativity, the spaceship hasn't actually moved relative to spacetime. Instead, the spaceship is always locally at rest because it has remained on the same part of the spring.

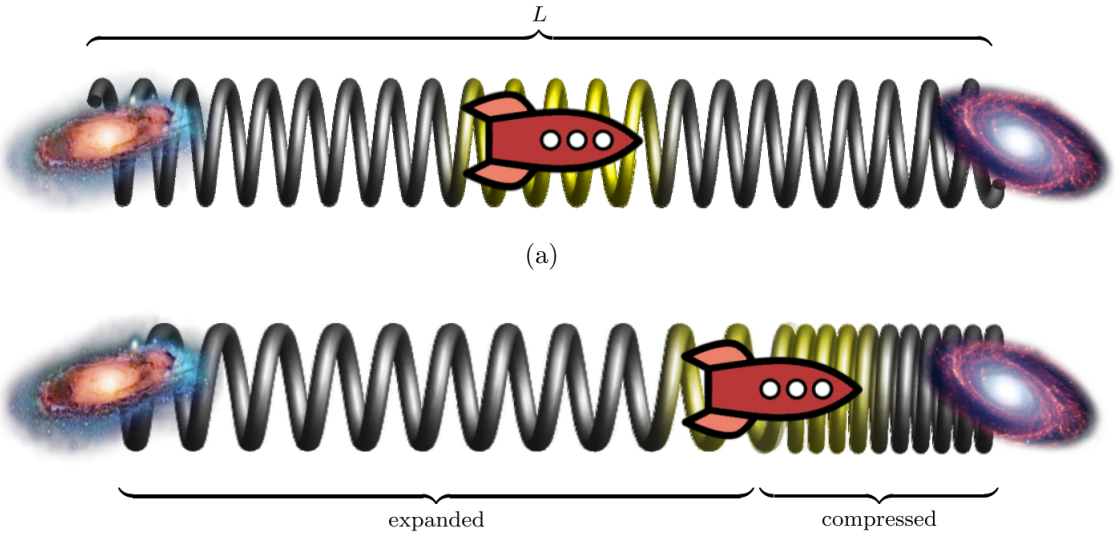

Figure 1.1: A qualitative analogy for the Alcubierre warp drive spacetime. Spacetime is represented by a stretchable spring. (a) A spaceship sits at rest with respect to spacetime. To reach the rightmost galaxy under ordinary conditions, the ship would have to travel a distance $L/2$ at a speed less than c. (b) In the Alcubierre warp drive, spacetime is expanded behind the spaceship and compressed in front of it. This is represented by a compression and expansion of the spring. To an outside observer, the ship appears to be traveling to the rightmost galaxy at a speed that is faster than light.

This provides a low-level illustration of the basic principles of the Alcubierre warp drive. The analogy is not exactly correct because an object in spacetime will not behave exactly like a point on a spring. As suggested by DeBenedictis [2], a better analogy might be a rigid plate moving through a compressible fluid. However, the spring is adequate for a basic qualitative introduction.

1.1.2 Properties of a Warp Drive

The Alcubierre warp drive has many interesting properties. First, an object inside the warp drive will experience no time dilation during its travel. In other words, the clock of someone at rest outside the warp drive and the clock of someone inside the warp drive would tick at the same rate. This is contrary to what one would expect from the perspective of special relativity. Second, the object inside the warp drive will not experience any tidal forces because the object remains on a locally flat and uncurved region of spacetime as it travels. The object will feel as if it is in free fall even though it appears to be accelerating to an outside observer.

These properties are presented here without evidence. A mathematically rigorous treatment will be given in Chapter 2.

1.2 Motivation

There are many motivations for studying the Alcubierre spacetime. The most obvious is the prospect of building a warp drive for space travel. Although many have argued that the warp drive cannot be physically realized [9] [10] [11], Alcubierre proposed that the the Casimir effect of quantum field theory could provide the necessary energy density to create a warp drive [8]. Several experiments have measured the Casimir force and have obtained results that are consistent with theoretical predictions [12] [13]. Modifications that would help ease the restrictive energy requirements of the spacetime have also been proposed [14].

Although a warp drive is beyond our current capabilities, it is not impossible that some other intelligent civilization has successfully constructed one. If so, it may be possible to detect a warp drive in the cosmos. Searches for so-called *technosignatures* of advanced cosmic technologies have been proposed for the Search for Extraterrestrial Intelligence (SETI) and other surveys [15] [16] [17]. It has also been suggested that technosignatures are the result of advanced space travel methods [18] [19]. What would a technosignature look like for a warp drive? It may be that an accelerating warp drive produces *Unruh radiation*, an emission of photons associated with an accelerating observer [20]. This is similar to the Hawking radiation produced by a black hole. Another possibility is that the expansion and contraction of spacetime in a warp drive could produce gravitational waves. Although these ideas are just speculation, a detailed study may reveal a potential technosignature of the warp drive.

As a third motivation, the Alcubierre spacetime provides an opportunity to study the physics of *horizons*. In the words of Rindler, a horizon is "a frontier between things observable and things unobservable" [21]. Many kinds of horizons have been studied: cosmological horizons, black hole horizons, and Rindler horizons for accelerated observers. As we will see in later chapters, a faster-than-light warp drive will create an *apparent horizon*. This is notable. Only a few solutions in general relativity have horizons that are time-dependent [22]. However, the apparent horizon of the warp drive depends explicitly on time. Therefore, the warp drive provides a unique opportunity to study the formation of an apparent horizon.

The final motivation for this project is personal. The science fiction author Arthur C. Clarke once said, "Any sufficiently advanced technology is indistinguishable from magic." Although this adage may be true for many futuristic technologies, it is not true for the warp drive because the warp drive has a precise mathematical description. It isn't magic; it is a perfectly valid solution in general relativity. This is enough to capture my curiosity and act as a motivation for this research.

1.2.1 Research Problem

What would a moving warp drive look like to someone on the outside? This is a natural question for both science fiction fans and physicists. Knowing the optical properties of the Alcubierre

spacetime would tell us what to look for when searching the cosmos. It would also be useful to compare the gravitational lensing and redshift effects of a warp drive to other spacetimes in general relativity.

Only a small number of papers have examined the optical properties of the Alcubierre spacetime. Clark et al. [23] presented the first detailed study of null geodesics in the warp drive spacetime in 1999. The approach was to numerically integrate the null geodesic equations to determine the redshift and angular deflection of photons passing through a warp drive. A paper by Müller et al. [24] provided a visualization of gravitational lensing effects. This was done numerically using four-dimensional ray-tracing techniques developed by the authors [25]. A third analysis of photon trajectories was performed by Anderson et al. [26] using an approach based on ray tracing in dielectric media [27] [28].

These studies have been restricted to numerical methods for calculating photon redshifts and trajectories. Currently, there is no analytic description of light propagation in the Alcubierre spacetime. This leaves an open question: how do electromagnetic waves propagate in a warp drive? This thesis will answer that question. The question is important because it could verify the numerical results of Clarke, Müller and Anderson. An analytic description could also reveal new insights into the redshift of photons and the 'apparent horizon' first predicted by Clark. Finally, an analytic approach would be novel and so might reveal yet-unexplored properties of this spacetime.

1.3 Overview of General Relativity

General relativity is a geometric theory of gravity. To unpack this statement, we must first discuss the fundamental tools and constructs that are used in general relativity. This section will present the conceptual framework and mathematical principles that will be used in this thesis.

1.3.1 Geometry & Spacetimes

Geometry plays a central role in general relativity. At the basic level, any geometry can be specified using a coordinate system and a line element. For instance, we can describe a flat two-dimensional plane using Cartesian coordinates (x, y). The Pythagorean theorem dictates that the distance ds between any two points on the plane will be

$$ds^2 = dx^2 + dy^2 \tag{1.2}$$

for some distances dx and dy. We could express the line element of Eq. (1.2) in any arbitrary coordinate system. This would yield a different equation for the line element but the new equation would still describe the geometry of a two-dimensional plane.

We can extend Eq. (1.2) to represent the geometry of a three-dimensional Euclidean space in

Cartesian coordinates (x, y, z) with the line element

$$ds^2 = dx^2 + dy^2 + dz^2. \tag{1.3}$$

Since this is the natural extension of the flat plane of Eq. (1.2), it is called *flat space*.

The theory of special relativity dictates that there is a different notion of time and simultaneity for every inertial frame. Combining space coordinates with time coordinates in our geometry gives rise to a new entity that is called *spacetime*. The simplest example of a spacetime is *flat spacetime* for which the line element takes the form

$$ds^2 = -(c\,dt)^2 + dx^2 + dy^2 + dz^2 \tag{1.4}$$

where c is the speed of light. The geometry that this line element represents is known as *Minkowski space*.

1.3.2 Mathematics of General Relativity

This section provides an overview of the basic mathematical constructions used in general relativity.

Four-Vectors

We will first start with a description of vectors. To describe dynamical quantities and distances, we must use vectors to connect two different points in spacetime. These objects are known as four-vectors. This name refers to the fact that there are four spacetime coordinates: three for space and one for time. A typical vector may be written

$$\boldsymbol{a} = \begin{pmatrix} a^0 \\ a^1 \\ a^2 \\ a^3 \end{pmatrix} = a^0\boldsymbol{e}_0 + a^1\boldsymbol{e}_1 + a^2\boldsymbol{e}_2 + a^3\boldsymbol{e}_3. \tag{1.5}$$

The quantities a^0, a^1, a^2, a^3 are called the components of the four-vector and the objects $\boldsymbol{e}_0$, $\boldsymbol{e}_1$, $\boldsymbol{e}_2$, $\boldsymbol{e}_3$ are called basis four-vectors. The basis four-vectors define a coordinate axis in an inertial frame. Any four-vector can be expressed as a linear combination of the basis four-vectors. By convention, components of a four-vector are specified using a superscript and basis vectors are labeled with a subscript.

Einstein Summation Convention

Upper and lower indices appear quite often in general relativity. It is useful to define a convention to simplify vector and tensor equations that involve many summations. If two indices of the same

letter appear in a subscript-superscript pair, summation over this index is implied. A repeated Latin index (such as i, j, k, ...) refers to a summation from 1 to 3 and a repeated Greek index (such as α, β, γ, ...) refers to a summation from 0 to 3. Using this convention, the right-hand side of Eq. (1.5) could be rewritten as

$$\boldsymbol{a} = \sum_{\alpha=0}^{3} a^{\alpha}\boldsymbol{e}_{\alpha} = a^{\alpha}\boldsymbol{e}_{\alpha} = a^{0}\boldsymbol{e}_{0} + a^{1}\boldsymbol{e}_{1} + a^{2}\boldsymbol{e}_{2} + a^{3}\boldsymbol{e}_{3}. \tag{1.6}$$

As illustrated in Eq. (1.6), the summation symbol Σ can be omitted from an expression and summation is still implied over the repeated indices.

Tensors

Tensors are common in general relativity. A tensor is a linear map from a set of vectors to a real number. To be precise, a tensor of rank r is a linear map from r vectors to a scalar quantity. A rank-2 tensor maps two vectors to a scalar, a rank-3 tensor maps three vectors to a scalar, and so on. A scalar can be considered a rank-0 tensor and a vector can be considered a rank-1 tensor. Like four-vectors, tensors are also assigned indices to specify their components. An example of a rank-3 tensor would be

$$s(a_{\alpha}, b^{\beta}, c^{\gamma}) = s^{\alpha}{}_{\beta\gamma}\, a_{\alpha}\, b^{\beta}\, c^{\gamma}. \tag{1.7}$$

The right-hand side of Eq. (1.7) implies a summation over all three indices and reduces the expression to a scalar quantity. The numbers $s^{\alpha}{}_{\beta\gamma}$ are called the components of the tensor s.

Metric Tensor

In the same way that we can define a line element ds^2 to describe Minkowski space in Eq. (1.4), we can describe all spacetimes in terms of some line element. The generalized line element has the form

$$ds^2 = g_{\mu\nu}\, dx^{\mu}\, dx^{\nu}. \tag{1.8}$$

Applying the Einstein summation convention, Eq. (1.8) becomes

$$\begin{aligned} ds^2 = {} & g_{00}\, dx^0\, dx^0 + g_{01}\, dx^0\, dx^1 + g_{02}\, dx^0\, dx^2 + g_{03}\, dx^0\, dx^3 + \\ & g_{10}\, dx^1\, dx^0 + g_{11}\, dx^1\, dx^1 + g_{12}\, dx^1\, dx^2 + g_{13}\, dx^1\, dx^3 + \\ & g_{20}\, dx^2\, dx^0 + g_{21}\, dx^2\, dx^1 + g_{22}\, dx^2\, dx^2 + g_{23}\, dx^2\, dx^3 + \\ & g_{30}\, dx^3\, dx^0 + g_{31}\, dx^3\, dx^1 + g_{32}\, dx^3\, dx^2 + g_{33}\, dx^3\, dx^3. \end{aligned} \tag{1.9}$$

The tensor $g_{\mu\nu}$ is known as the *metric tensor* (sometimes shortened to just *metric*) with components g_{00}, g_{01}, g_{02}, ..., g_{33}. The metric is a rank-2 tensor that maps any two four-vectors to a scalar quantity that is equal to their inner product. While $g_{\mu\nu}$ will have different components in

different coordinate systems, the quantity ds^2 will be invariant.

The metric tensor can be represented as the matrix

$$g_{\mu\nu} = \begin{pmatrix} g_{00} & g_{01} & g_{02} & g_{03} \\ g_{10} & g_{11} & g_{12} & g_{13} \\ g_{20} & g_{21} & g_{22} & g_{23} \\ g_{30} & g_{31} & g_{32} & g_{33} \end{pmatrix}. \tag{1.10}$$

For a four-dimensional spacetime, this matrix will always be 4×4 and symmetric. Any line element can be cast in the form of a matrix. For instance, by comparing Eq. (1.4) to Eq. (1.8), it can be seen that the Minkowski line element has $g_{00} = -1$, $g_{11} = g_{22} = g_{33} = 1$ (using the convention of setting $c = 1$). Therefore, the metric tensor for Minkowski space can be written in matrix form as

$$g_{\mu\nu} = \begin{pmatrix} -1 & 0 & 0 & 0 \\ 0 & 1 & 0 & 0 \\ 0 & 0 & 1 & 0 \\ 0 & 0 & 0 & 1 \end{pmatrix}. \tag{1.11}$$

This is one of the simplest examples of a metric tensor; all entries are constant and the matrix is diagonal. In general, the metric for an arbitrary spacetime will be a function of the coordinate variables and may have off-diagonal elements.

The metric can be used to raise or lower indices of a vector or tensor. To turn a contravariant vector into a covariant vector, the contravariant vector components transform according to

$$a_\alpha = g_{\alpha\beta}\, a^\beta. \tag{1.12}$$

In a similar manner, the components of a covariant vector can be transformed using the *inverse metric*, $g^{\alpha\beta}$:

$$a^\alpha = g^{\alpha\beta}\, a_\beta. \tag{1.13}$$

The inverse metric is defined by the relation

$$g^{\alpha\gamma} g_{\gamma\beta} = \delta^\alpha_\beta. \tag{1.14}$$

Geodesic Motion

In Newtonian mechanics, the dynamics of a particle are governed by the variational principle. The variational principle states that a particle will move between one point in space (x_0, y_0, z_0) at time t_0 and another point in space (x, y, z) at a later time t in a way that extremizes the action

S. This statement gives rise to the Lagrangian equation of motion

$$-\frac{d}{dt}\left(\frac{\partial L}{\partial \dot{x}^a}\right)+\frac{\partial L}{\partial x^a}=0. \tag{1.15}$$

that governs classical dynamics.

In an analogous way, the dynamics of a particle in a curved spacetime can be derived from a variational principle. The variational principle for curved spacetime states that the worldline of a free test particle between two timelike points will be the path that extremizes the proper time τ between them. Mathematically, the proper time between two points is

$$\tau_{AB}=\int_A^B d\tau=\int_A^B \sqrt{-g_{\mu\nu}\,dx^\mu\,dx^\nu}. \tag{1.16}$$

If the path of the particle is parametrized by λ so that $\lambda=0$ at point A and $\lambda=1$ at point B, then Eq. (1.16) becomes

$$\tau_{AB}=\int_0^1 \sqrt{-g_{\mu\nu}\frac{dx^\mu}{d\lambda}\frac{dx^\nu}{d\lambda}}\,d\lambda. \tag{1.17}$$

The proper time between A and B is then minimized when the worldlines $x^\mu(\lambda)$ and $x^\nu(\lambda)$ satisfy the Lagrange equation

$$-\frac{d}{d\lambda}\left(\frac{\partial L}{\partial\left(dx^\mu/d\lambda\right)}\right)+\frac{\partial L}{\partial x^\mu}=0 \tag{1.18}$$

for the Lagrangian

$$L=\sqrt{-g_{\mu\nu}\frac{dx^\mu}{d\lambda}\frac{dx^\nu}{d\lambda}}. \tag{1.19}$$

If the equations of motion are calculated explicitly for a given curved spacetime from Eq. (1.18), they will be of the form

$$\frac{d^2x^\alpha}{d\tau^2}=-\Gamma^\alpha_{\beta\gamma}\frac{d^2x^\beta}{d\tau^2}\frac{d^2x^\gamma}{d\tau^2} \tag{1.20}$$

where $\Gamma^\alpha_{\beta\gamma}$ are called the *Christoffel symbols*. The Christoffel symbols (also known as the *connection*) can be calculated from the metric tensor according to

$$g_{\alpha\delta}\,\Gamma^\delta_{\beta\gamma}=\frac{1}{2}\left(\frac{\partial g_{\alpha\beta}}{\partial x^\gamma}+\frac{\partial g_{\alpha\gamma}}{\partial x^\beta}-\frac{\partial g_{\beta\gamma}}{\partial x^\alpha}\right). \tag{1.21}$$

The Christoffel symbols are symmetric in the lower two indices: $\Gamma^\delta_{\beta\gamma}=\Gamma^\delta_{\gamma\beta}$.

Eq. (1.20) is known as the *geodesic equation*. Free particles that are only influenced by spacetime curvature (that is, free from all external forces) are said to be traveling on *geodesic lines*. From a Newtonian perspective we would say that the particle is only influenced by gravitational force. From the perspective of general relativity this statement wouldn't be exactly correct; the gravitational interaction is not a force but a consequence of spacetime curvature. We therefore say a particle is freely-falling when its motion obeys the geodesic equation.

Covariant Derivative

It is useful to differentiate vectors in general relativity. The derivative of a vector will naturally require the difference between vectors at adjacent points in spacetime. This is problematic because the subtraction of vectors is only defined at a single point (that is, a common *tangent space*). It is therefore necessary to transport vectors from one spacetime point to another if we wish to properly define a vector derivative.

Consider two vectors v and v' at two different spacetime points x^α and $x^\alpha + \Delta^\alpha$. To construct the derivative, the vector v' is transported to the point x^α in a manner parallel to itself. This transported vector is then called v_{PT}. The difference between the vectors v and v_{PT} can now be computed because they are defined at the same point (they are defined in the tangent space of x^α). With parallel transport the derivative of a vector field $\boldsymbol{v}(x^\alpha)$ can be computed using the *covariant derivative*,

$$\boldsymbol{\nabla_t v}\left(x^\alpha\right) = \lim_{\epsilon \to 0} \frac{\left[\boldsymbol{v}(x^\alpha + t^\alpha \epsilon)\right]_{\mathrm{PT}} - \boldsymbol{v}(x^\alpha)}{\epsilon}. \tag{1.22}$$

In general, it is necessary to modify Eq. (1.22) for the cases where the components of the vector change under parallel transport. An illustration of how vector components change under parallel transport is given in Fig. 1.2. We can account for the change in the angle between the vector and the basis vectors using the general covariant derivative,

$$\nabla_\beta \, v^\alpha = \frac{\partial v^\alpha}{\partial x^\beta} + \Gamma^\alpha_{\beta\gamma} \, v^\gamma, \tag{1.23}$$

where the Christoffel symbols $\Gamma^\alpha_{\beta\gamma}$ are as in Eq. (1.21).

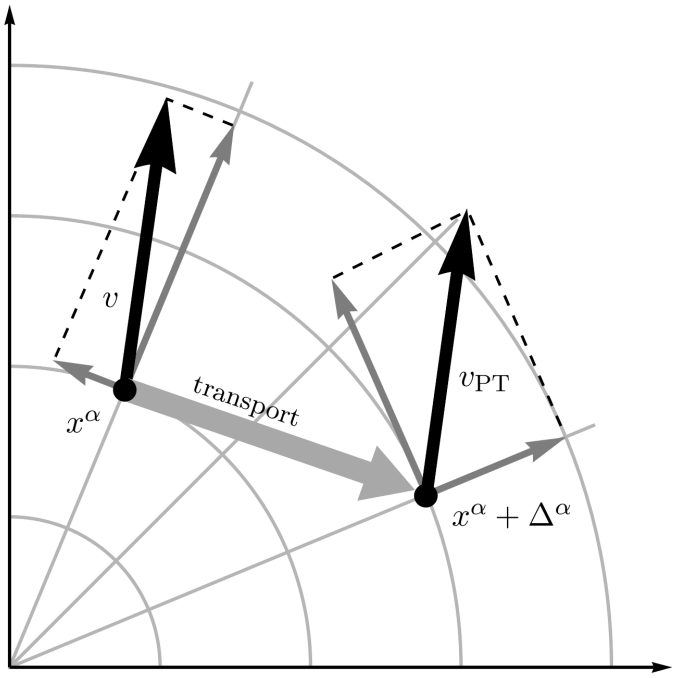

Figure 1.2: Vector components change under parallel transport. In two-dimensional polar coordinates, the $\hat{r}$ and $\hat{\theta}$ components of the vector v are different from those of the transported vector v_{PT} under a translation $x^\alpha \to x^\alpha + \Delta^\alpha$. This situation is analogous to parallel transport in a curved spacetime.

Chapter 2

Alcubierre Metric

In the Alcubierre warp drive, an object can achieve large apparent speeds due to the expansion and contraction of spacetime. This expansion and contraction can be described in terms of a metric tensor known as the *Alcubierre metric*. Building on the qualitative description of Section 1.1.1, this chapter will present the mathematics of the warp drive.

2.1 Definition of the Alcubierre Metric

Consider an object lying in the x-t plane of a Cartesian coordinate system. We wish to define a metric tensor that will 'push' the object from behind and 'pull' it forward so that it moves in the $\hat{x}$ direction. In other words, the object is inside a warp drive moving in the $\hat{x}$ direction. To an outside observer, we would like the object to appear to be traveling along a parametric path given by $x = x_{\rm o}(t)$, $y = 0$, $z = 0$. We choose the subscript 'o' to indicate that this is the trajectory for an *object* traveling in the warp drive. The velocity associated with this trajectory is $V(t) \equiv dx_{\rm o}(t)/dt$. It is important to note that $V(t)$ is not bounded by the speed of light and can have any value. This allows for apparent faster-than-light travel. A metric tensor that has these "warp drive" characteristics is given by

$$ds^2 = -dt^2 + [dx - V(t)\, f(r_{\rm o})\, dt]^2 + dy^2 + dz^2 \tag{2.1}$$

This is the *Alcubierre metric*. It was found by Miguel Alcubierre in 1994 [8]. In this metric, $r_{\rm o} \equiv ((x - x_{\rm o}(t))^2 + y^2 + z^2)$ is the spatial distance from the object in the warp drive. The object is defined to be at $r_{\rm o} = 0$ which corresponds to the center of the warp drive. The function $f(r_{\rm o})$ is called the *shaping function*. It is a smooth and positive function that satisfies $f(0) = 1$ and $f \to 0$ for increasing $r_{\rm o}$. This function is typically taken to be

$$f(r_{\rm o}) = \frac{\tanh\left(\sigma\left(r_{\rm o}(t) + R\right)\right) - \tanh\left(\sigma\left(r_{\rm o}(t) - R\right)\right)}{2\tanh\left(\sigma R\right)} \tag{2.2}$$

where R and σ are arbitrary parameters that we assume to be positive. How can we interpret this function? It describes a region of flat spacetime inside the warp drive that is called the *warp bubble*. The warp bubble surrounds the object in the warp drive and acts as a kind of "boundary" that separates everything inside the warp drive and everything that is outside. The parameter R defines the radius of the warp bubble. In other words, the boundary of the warp drive is a distance

R away from the center of the warp drive ($r_o = 0$). The parameter σ defines the "sharpness" of the boundary of the warp bubble. This can be seen in Fig. 2.1.

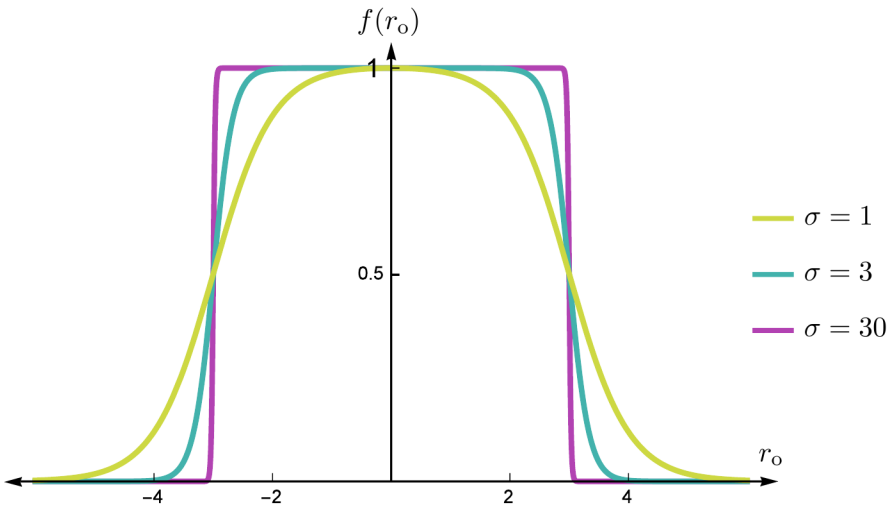

Figure 2.1: The shaping function (Eq. (2.2)) for $R = 3$ and various σ. This function defines a central region of flat spacetime inside the warp drive that is called the *warp bubble*. The warp bubble is defined to be the region where $f(r_o) \approx 1$. Ordinary flat spacetime surrounds the warp bubble. This corresponds to regions where $f(r_o) \approx 0$. The parameter σ defines the "sharpness" of the boundary between the warp bubble and the rest of the universe.

In the limit where σ is very large, $f(r_o)$ rapidly approached the "top-hat" function:

$$\lim_{\sigma\to\infty} f(r_o) = \begin{cases} 1, & r_o \in (-R, R) \\ 0, & \text{else} \end{cases} \tag{2.3}$$

We can rewrite Eq. (2.1) in the form of a 4×4 matrix. Expanding the line element in the second term yields

$$ds^2 = (V(t)^2\, f(r_o)^2 - 1)\, dt^2 - 2\, V(t)\, f(r_o)\, dx\, dt + dx^2 + dy^2 + dz^2. \tag{2.4}$$

The elements of the matrix can now be read off using Eq. (1.8). To find the off-diagonal elements, we can exploit the symmetry of the metric: $g_{\mu\nu} = g_{\nu\mu}$. This allows us to write

$$\begin{aligned} -2\, V(t)\, f(r_o) &= g_{01}\, dx\, dt + g_{10}\, dx\, dt \\ &= dx\, dt\, (g_{01} + g_{10}) \\ &= 2\, dx\, dt\, g_{01} \end{aligned} \tag{2.5}$$

which implies $g_{10} = g_{01} = -V(t)f(r_o)$. In matrix form, the Alcubierre metric is

$$g_{\alpha\beta} = \begin{pmatrix} V(t)^2 f(r_o)^2 - 1 & -V(t) f(r_o) & 0 & 0 \\ -V(t) f(r_o) & 1 & 0 & 0 \\ 0 & 0 & 1 & 0 \\ 0 & 0 & 0 & 1 \end{pmatrix}. \tag{2.6}$$

2.2 Properties of the Alcubierre Metric

The most startling property of the Alcubierre metric is that it allows for apparent faster-than-light motion. It is well known that faster-than-light motion is forbidden by special relativity. It is also forbidden in the context of general relativity but with one important caveat: in general relativity, nothing can travel faster than the speed of light *locally*. Although the object in the warp drive may appear to be traveling at a speed greater than c to an outside observer, it never actually exceeds the speed of light in its local frame. This can be shown by calculating the light cones for the Alcubierre metric. Consider a warp drive in two dimensions that moves in the $\hat{x}$ direction. The metric is then given by

$$ds^2 = -dt^2 + [dx - V(t)\, f(r_o)\, dt]^2. \tag{2.7}$$

The light cones correspond to spacetime intervals for which $ds^2 = 0$:

$$0 = (V(t)^2\, f(r_o)^2 - 1)\, dt^2 - 2\, V(t)\, f(r_o)\, dx\, dt + dx^2. \tag{2.8}$$

Solving for dx/dt, we find

$$\frac{dx}{dt} = \pm 1 + V(t)\, f(r_o). \tag{2.9}$$

This governs the behaviour of light cones in the Alcubierre spacetime (we have set $c = 1$, which we will do for the rest of this thesis). The object inside the warp drive is always defined to be at $r_o = 0$. This corresponds to $f(r_o) = 1$ so the previous equation becomes

$$\frac{dx}{dt} = \pm 1 + V(t). \tag{2.10}$$

Since $V(t)$ is the velocity of the object, we can conclude that

$$V(t) - 1 < V(t) < V(t) + 1. \tag{2.11}$$

In other words, the object inside the warp drive is always within its local light cone. Although it may appear that the object is traveling faster than light to an outside observer, this is only because the light cones are now "tipped". On a spacetime diagram, the light cones are lines with slopes given by Eq. (2.9).

Another interesting property is that the object in the warp drive will feel as if it is in free fall. Despite the extreme expansion and contraction of spacetime around it, the object will experience no tidal forces because the warp bubble is a region of flat spacetime. To illustrate, consider the region near $r_{\mathrm{o}} = 0$ (i.e. the center of the warp bubble). In this region, Eq. (2.2) and Fig. 2.1 show that $f(r_{\mathrm{o}}) \approx 1$. Plugging this into the metric tensor yields

$$g_{\alpha\beta} = \begin{pmatrix} V(t)^2 - 1 & -V(t) & 0 & 0 \\ -V(t) & 1 & 0 & 0 \\ 0 & 0 & 1 & 0 \\ 0 & 0 & 0 & 1 \end{pmatrix}. \tag{2.12}$$

If $V(t)$ is taken to be constant then all the matrix elements of Eq. (2.12) are constant and the Christoffel symbols vanish. This means that the object is undergoing geodesic motion. Hence, the object feels as if it is in free fall.

What about points that are far away from the warp bubble? In this situation, r_{o} is large and so $f(r_{\mathrm{o}}) \approx 0$. The metric tensor reduces to

$$g_{\alpha\beta} = \begin{pmatrix} -1 & 0 & 0 & 0 \\ 0 & 1 & 0 & 0 \\ 0 & 0 & 1 & 0 \\ 0 & 0 & 0 & 1 \end{pmatrix} \tag{2.13}$$

which is just the metric for Minkowski space. Thus, everything outside the warp bubble corresponds to flat spacetime.

A third interesting property is that the proper time of an object in the warp drive is equal to the coordinate time. From the perspective of special relativity, this is unusual because one would expect a rapidly-moving object to undergo time dilation. To show that the proper time τ is equal to the coordinate time T, we can use the definition of proper time:

$$\begin{aligned} \tau &= \int_0^T -g_{\alpha\beta}\, dx^\alpha\, dx^\beta \\ &= \int_0^T (dt^2 - [dx - V(t)\, f(r_{\mathrm{o}})\, dt]^2)^{1/2} \end{aligned} \tag{2.14}$$

For an object at the center of the warp bubble, $f(r_{\mathrm{o}}) \approx 1$. The object velocity is defined as

$V(t) = dx/dt$. Thus, the proper time reduces to

$$\begin{aligned} \tau &= \int_0^T (dt^2 - [dx - \frac{dx}{dt}\, dt]^2)^{1/2} \\ &= \int_0^T (dt^2)^{1/2} \\ &= T. \end{aligned} \tag{2.15}$$

This shows that the object inside the warp drive would experience no time dilation relative to an outside observer at rest.

Finally, it is important to discuss whether the Alcubierre metric is a physical spacetime. The Einstein field equation implies that the Alcubierre metric requires negative energy densities. Unfortunately, the energy densities of all known classical fields are positive. Although there are quantum fields that would permit negative energy densities [29], many have argued that the Alcubierre metric does not correspond to a physically realizable spacetime [10] [11] [30]. Pfenning and Ford [9] have also argued that even if negative energy densities could be physically sustained, there would be other restrictions on the size and thickness of the warp bubble. Further study has shown that apparent superluminal travel will violate the weak energy condition of general relativity [31] [32]. However, there has been work that has shown a warp drive is possible with less restrictive energy requirements [14].

2.3 Wave Equation for the Alcubierre Metric

We are interested in describing the propagation of electromagnetic waves. The natural starting point for this problem is to derive the electromagnetic wave equation for the Alcubierre metric. It happens that there is a form for the wave equation in an arbitrary curved spacetime [33]. The wave equation without source terms is

$$\Box A^\mu = 0 \tag{2.16}$$

where A^μ is the electromagnetic four-potential. The operator $\Box$ is the *d'Alembert operator* and is defined as

$$\Box = \nabla_\mu \nabla^\mu = g^{\mu\nu}\, \nabla_\mu \nabla_\nu \tag{2.17}$$

with ∇_β representing the covariant derivative operator. Applying the covariant derivative operator twice to A^μ will make for a complicated derivation. To simplify the problem, we can instead consider a scalar field ϕ instead of a vector field A^μ. The covariant derivative of a scalar field is

equivalent to the partial derivative and so the wave equation becomes

$$\begin{aligned}\nabla_\mu \nabla^\mu \,\phi &= g^{\mu\nu}\,\nabla_\mu \nabla_\nu\,\phi \\ &= g^{\mu\nu}\,\nabla_\mu\,\partial_\nu\,\phi \\ &= g^{\mu\nu}\,\partial_\mu\,\partial_\nu\,\phi - g^{\mu\nu}\,\Gamma^\sigma_{\nu\mu}\,\partial_\sigma\,\phi \\ &= (\partial_\mu\partial^\mu - g^{\mu\nu}\,\Gamma^\sigma_{\nu\mu}\,\partial_\sigma)\,\phi\end{aligned} \tag{2.18}$$

where we have applied the definition

$$\nabla_\beta \lambda_\alpha \equiv \partial_\beta \lambda_\alpha - \Gamma^\gamma_{\beta\alpha}\lambda_\gamma. \tag{2.19}$$

The Alcubierre metric has the inverse

$$g^{\mu\nu} \;=\; \begin{pmatrix} -1 & -V(t)f(r_{\rm o}) & 0 & 0 \\ -V(t)f(r_{\rm o}) & 1-V(t)^2 f(r_{\rm o})^2 & 0 & 0 \\ 0 & 0 & 1 & 0 \\ 0 & 0 & 0 & 1 \end{pmatrix} \tag{2.20}$$

We can easily calculate the Christoffel symbols using a Mathematica package. The explicit form of the Christoffel symbols is given in Appendix A. The wave equation reduces to

$$\begin{aligned}\nabla_\mu \nabla^\mu \phi = \Big(&- \frac{\partial^2}{\partial (x^0)^2} + \frac{\partial^2}{\partial (x^2)^2} + \frac{\partial^2}{\partial (x^3)^2} - 2\,f\,V \frac{\partial}{\partial x^0}\frac{\partial}{\partial x^1} + \left(1 - f^2 V^2\right) \frac{\partial^2}{\partial (x^1)^2} \\ &+ f\left(\frac{\partial V}{\partial x^0} + 2\,V^2 \frac{\partial f}{\partial x^1}\right)\frac{\partial}{\partial x^1} + V \frac{\partial f}{\partial x^1}\frac{\partial}{\partial x^0}\Big)\,\phi\end{aligned} \tag{2.21}$$

where we have used the notation $x^0 = t$, $x^1 = x$, $x^2 = y$, $x^3 = z$. Although the wave equation can be found, it is difficult to solve analytically in the original x-t coordinate system. A different approach may be better suited to our problem.

Chapter 3

Wave Equation in Conformally Flat Coordinates

The goal of this research is to develop an analytic description of electromagnetic wave propagation in the Alcubierre spacetime. As we saw in Section 2.3, the wave equation is complicated and difficult to solve analytically in the original x-t coordinate system. Instead, we seek an alternative method to describe wave propagation. Our approach is to find a coordinate transformation that makes the Alcubierre metric conformally flat.

3.1 Overview of Conformal Transformations

A *conformal transformation* is a point-dependent rescaling of a metric tensor. A conformal transformation expands or shrinks the distances between spacetime points in a coordinate system x^α while locally preserving the angles between vectors. A metric that has undergone a conformal transformation takes the form

$$g'_{\mu\nu}(x) = \Omega^2(x)\, g_{\mu\nu}(x). \tag{3.1}$$

This is known as a *conformally equivalent metric*. It is related to the original metric through a change of coordinates. Here, Ω is a smooth and continuous function that is called the *conformal factor*. This factor describes the rescaling of the metric at each spacetime point and so it is a function of the coordinates. The conformal transformation of Eq. (3.1) can equivalently be written in terms of the line element:

$$(ds')^2 = \Omega^2(x)\, ds^2. \tag{3.2}$$

The conformal factor is written $\Omega^2(x)$ instead of $\Omega(x)$ so that the conformal factor is always positive. This limits the transformations to those where the sign of ds^2 remains unchanged. Thus, spacelike intervals remain spacelike and timelike intervals remain timelike.

Conformal transformations are generally different from coordinate transformations. A conformal transformation implies that the line element, which measures the distance between spacetime points, will change from point to point in spacetime. There is no reference to direction and so the conformal scaling can be called *isotropic*. This means that the angle between vectors doesn't change but the distance between nearby points does change. This is precisely why the term

"conformal" is used.

To illustrate the concept of conformal transformations, it is useful to consider the simplest case of $\Omega(x) = \Omega =$ constant. In this case, the line element changes identically at all points in spacetime. This is called a *scale transformation* because it scales the metric everywhere by a constant. It is also referred to as a *global transformation* because the scaling is independent of the coordinate representation of the metric. Extending this simple case, we can say that a general conformal transformation is a *localized scale transformation* because it assigns a scale transformation for each spacetime point. In this context, it is intuitive why the conformal factor $\Omega^2(x)$ is a function of the coordinates: we are changing how distances are measured at each spacetime point. The transformation to the new metric $g'_{\mu\nu}$ is said to be a transformation to a new *conformal frame*.

Any two-dimensional metric is conformally equivalent to the two-dimensional Minkowski metric [34]. To state it another way, one can always find a set of coordinates in which the two-dimensional metric looks like the Minkowski metric multiplied by a conformal factor $\Omega^2(x)$:

$$g'_{\mu\nu}(x) = \Omega^2(x) \begin{pmatrix} -1 & 0 \\ 0 & 1 \end{pmatrix}. \tag{3.3}$$

This is known as *conformal flatness*. Note that conformal flatness does not imply that the metric is equivalent to the Minkowski metric. It only says that there exists a mapping from the curved spacetime to Minkowski space that preserves angles. Conformal flatness is extremely useful for our purposes. We wish to solve the wave equation in the Alcubierre metric but this is difficult to do in the original coordinate system. However, since every two-dimensional metric is conformally equivalent to the Minkowski metric, we can find a coordinate transformation that reduces the Alcubierre metric to the conformally flat metric of Eq. (3.3). Once we are in these new coordinates, we can solve the wave equation easily. Why? The wave equation in a conformally flat metric takes the form

$$\Omega^2 \left(\partial^2_{w^0} - \partial^2_{w^1}\right) \phi(w^0, w^1) = 0 \tag{3.4}$$

with solutions

$$\phi(w^0, w^1) = F(w^1 - w^0) + G(w^1 + w^0). \tag{3.5}$$

If we can find the conformal coordinates in which the Alcubierre metric takes the form of Eq. (3.3) then we can propagate the wave according to Eq. (3.5). After doing so, we can transform back to our original coordinates to get a picture of how electromagnetic waves propagate everywhere in the Alcubierre spacetime. Ultimately, our goal is to find a conformal coordinate transformation that will allow us to do this.

3.2 Conformally Flat Coordinates for the Alcubierre Metric

To start, we consider the Alcubierre metric in two-dimensions,

$$g_{\alpha\beta} = \begin{pmatrix} V(x^0)^2 f(x^1 - V(x^0)\,x^0)^2 - 1 & -V(x^0)\,f(x^1 - V(x^0)\,x^0) \\ -V(x^0)\,f(x^1 - V(x^0)\,x^0) & 1 \end{pmatrix}, \tag{3.6}$$

where we have used the convention $t = x^0$, $x = x^1$. Since the warp drive is expanding and contracting spacetime along the $\hat{x}$ direction, the y and z coordinates can be excluded from the metric tensor without losing the essential properties of the warp drive. Thus, Eq. (3.6) is an adequate description of a two-dimensional warp drive. Next, we assume the case of a warp drive moving at constant velocity. Although an accelerating warp drive would be a more general problem to solve, we will limit ourself to $V(t) = V =$ constant in this section. We also simplify the problem by defining a "one-sided shaping function" $f(x^0, x^1)$. This function divides space into two regions: one region corresponds to inside the warp bubble and the other corresponds to outside the warp bubble. For the constant-V case, this one-sided shaping function $f(x^0, x^1)$ is defined as

$$f(x^0, x^1) = f(x^1 - Vx^0) = \frac{1 + \tanh(\sigma(x^1 - Vx^0))}{2}. \tag{3.7}$$

Graphically, $f(x^0, x^1)$ looks as in Fig. 3.1.

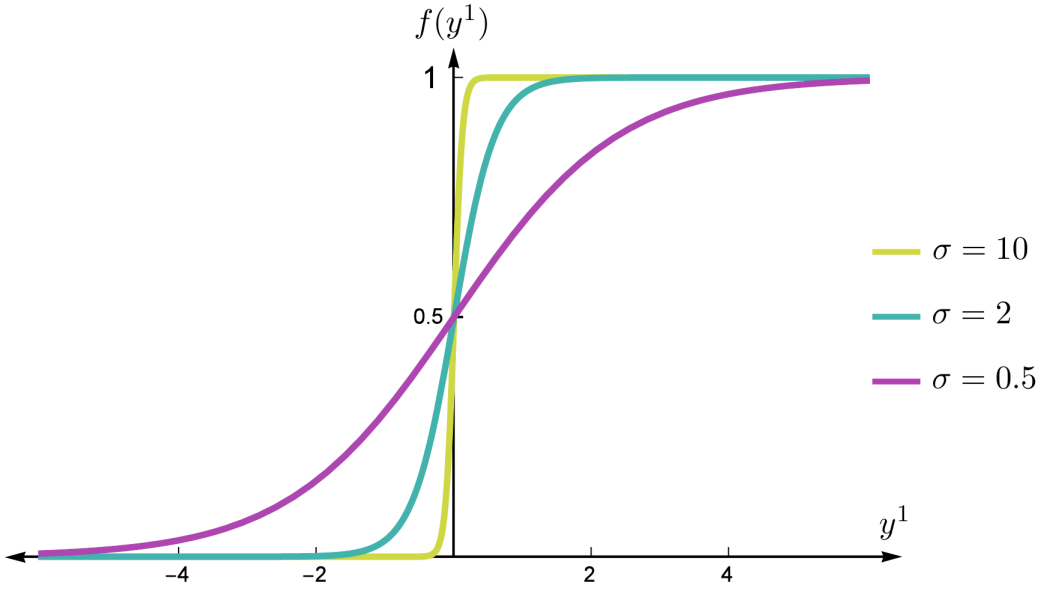

Figure 3.1: The one-sided shaping function $f(y^1)$ for various σ. The substitution $y^1 = x^1 - Vx^0$ has been made. This function divides spacetime into two regions: one in which we are inside the warp drive and one in which we are outside. As was the case in Fig. 2.1, the parameter σ affects the "sharpness" of the boundary of the warp bubble.

The goal is to find a coordinate transformation that will put the Alcubierre metric in the form of Eq. (3.3). To do so, we first make a change of variables to the *comoving frame* of the warp bubble. This is a transformation to a reference frame that is moving alongside the warp drive at the same speed V. The new coordinates are y^0, y^1 and the coordinate transformation is defined as

$$\begin{aligned} y^0 &= x^0 \\ y^1 &= x^1 - Vx^0. \end{aligned} \tag{3.8}$$

We can then transform the metric according to

$$g_{\alpha'\beta'} = \frac{\partial x^\gamma}{\partial x^{\alpha'}} \frac{\partial x^\delta}{\partial x^{\beta'}} g_{\gamma\delta}. \tag{3.9}$$

The Jacobi matrix for this transformation is

$$J = \begin{pmatrix} 1 & 0 \\ V & 1 \end{pmatrix} \tag{3.10}$$

and the determinant is non-zero so the transformation is invertible. The new metric is

$$g_{\alpha'\beta'} = \begin{pmatrix} -1 + \frac{V^2}{\left(1+e^{2y^1\sigma}\right)^2} & \frac{V}{1+e^{2y^1\sigma}} \\ \frac{V}{1+e^{2y^1\sigma}} & 1 \end{pmatrix}. \tag{3.11}$$

We next introduce an x^1-dependent shift of the coordinates to diagonalize the metric. To do so, we first go to a new set of coordinates z^0, z^1:

$$\begin{aligned} z^0 &= y^0 - q(y^1) \\ z^1 &= y^1 \end{aligned} \tag{3.12}$$

where $q(y^1)$ is some yet-undetermined function. This coordinate transformation yields a metric of the form

$$g_{\alpha'\beta'} = \begin{pmatrix} -1 + \xi^2 & \xi + \left(-1+\xi^2\right) q'(z^1) \\ \xi + \left(-1+\xi^2\right) q'(z^1) & 1 + 2\xi q'(z^1) + \left(-1+\xi^2\right) q'(z^1)^2 \end{pmatrix} \tag{3.13}$$

where $\xi \equiv \frac{V}{1+e^{2z^1\sigma}}$. In this form, we can attempt to find a function $q(z^1)$ that will make the off-diagonal elements of metric disappear. By looking at Eq. (3.13), we find that this occurs when $q'(z^1)$ takes the form

$$q'(z^1) = \frac{\left(1+e^{2z^1\sigma}\right)V}{1 + 2e^{2z^1\sigma} + e^{4z^1\sigma} - V^2}. \tag{3.14}$$

Integrating this equation, we arrive at a functional form for $q(z^1)$:

$$\begin{aligned} q(z^1) = &\frac{V(-4z^1\sigma - (-1+V)\log(1+e^{2z^1\sigma}+V)}{4(-1+V^2)\sigma} \\ &+ \frac{(1+V)\log|1+e^{2z^1\sigma}-V|)}{4(-1+V^2)\sigma}. \end{aligned} \tag{3.15}$$

It is notable that the function is undefined when $V = 1$. Now that we have an explicit functional form for $q(z^1)$, we can perform the coordinate transformation. The new metric has the form

$$g_{\alpha'\beta'} = \begin{pmatrix} -1 + \frac{V^2}{(1+e^{2z^1\sigma})^2} & 0 \\ 0 & \frac{1}{1-\frac{V^2}{(1+e^{2z^1\sigma})^2}} \end{pmatrix} \tag{3.16}$$

and it is indeed diagonal. The final step is to rescale the z^1 coordinate of the transformation to find the conformal factor Ω^2. In order to avoid dealing with inverse functions, we perform this final coordinate transformation using the inverse metric. The inverse of the previous metric is given by

$$g^{\alpha'\beta'} = \begin{pmatrix} \frac{1}{-1+\frac{V^2}{\left(1+e^{2z^1\sigma}\right)^2}} & 0 \\ 0 & 1 - \frac{V^2}{\left(1+e^{2z^1\sigma}\right)^2} \end{pmatrix}. \tag{3.17}$$

We define a new transformation to try to do this "rescaling",

$$w^0 = z^0 \tag{3.18}$$

$$w^1 = g(z^1). \tag{3.19}$$

Now transforming the metric, we arrive at

$$g_{\alpha'\beta'} = \begin{pmatrix} \frac{1}{-1+\frac{V^2}{(1+e^{2z^1\sigma})^2}} & 0 \\ 0 & g'(z^1)^2\big(1 - \frac{V^2}{(1+e^{2z^1\sigma})^2}\big) \end{pmatrix} \tag{3.20}$$

After some calculation, we can find the expression for $w^1 = g(z^1)$. This is given by

$$\begin{aligned} g(z^1) = w^1(z^1) = &- \frac{z^1}{(-1+V)(1+V)} + \frac{V\log\left|1+e^{2z^1\sigma}-V\right|}{4(-1+V)\sigma} \\ &+ \frac{V\log\left(1+e^{2z^1\sigma}+V\right)}{4(1+V)\sigma}. \end{aligned} \tag{3.21}$$

With this coordinate transformation, the new metric is

$$g_{\alpha'\beta'} = \begin{pmatrix} -1 + \frac{V^2}{(1+e^{2z^1\sigma})^2} & 0 \\ 0 & 1 - \frac{V^2}{(1+e^{2z^1\sigma})^2} \end{pmatrix}. \tag{3.22}$$

and we have accomplished our goal. This metric is conformally equivalent to the Minkowski metric. Factoring our the conformal factor, we arrive at

$$g_{\alpha'\beta'} = \left(1 - \frac{V^2}{(1+e^{2z^1\sigma})^2}\right) \begin{pmatrix} -1 & 0 \\ 0 & 1 \end{pmatrix} \tag{3.23}$$

and so the conformal factor is

$$\Omega^2 = 1 - \frac{V^2}{(1+e^{2z^1\sigma})^2}. \tag{3.24}$$

In summary, the transformation is

$$\begin{array}{lll} x^0 = y^0 & y^0 = z^0 + q(z^1) & z^0 = w^0 \\ x^1 = y^1 + V\,y^0 & y^1 = z^1 & z^1 = g^{-1}(w^1) \end{array} \tag{3.25}$$

The full transformation from $x^\alpha \to w^\alpha$ can now be found by performing the required coordinate transformations in series. The transformation for w^1 is given by Eq. (3.21). The transformation for w^0 is given by

$$w^0(x^0,\, x^1) = z^0 = y^0 - q(y^1) = x^0 - q(x^1 - V\,x^0). \tag{3.26}$$

Explicitly, this transformation looks like

$$\begin{aligned} w^0(x^0,\, x^1) = x^0 &+ \frac{V\left(-Vx^0 + x^1\right)}{-1+V^2} \\ &+ \frac{V(-1+V)\log\left(1 + e^{2(-Vx^0+x^1)\sigma} + V\right)}{4\sigma\left(-1+V^2\right)} \\ &- \frac{V(1+V)\log\left|1 + e^{2(-Vx^0+x^1)\sigma} - V\right|}{4\sigma\left(-1+V^2\right)}. \end{aligned} \tag{3.27}$$

Thus, we have found the exact coordinate transformations between w^α and x^α that will reduce the two-dimensional Alcubierre metric of Eq. (3.6) to the conformally flat metric of Eq. (3.3).

3.3 Approximate Transformations

The exact coordinate transformations found in the previous section will allow us to transform from our original x^α coordinates to a new set of coordinates w^α where the metric is conformally flat. Unfortunately, these coordinate transformations are not invertible. Due to the logarithmic terms,

we cannot find an exact expression for $x^0(w^0, w^1)$ and $x^1(w^0, w^1)$. Instead, it is necessary to find approximate coordinate transformations if we wish to transform back to the original coordinates.

I will illustrate the procedure for finding these approximate coordinate transformations using $w^1(x^0, x^1)$ and assuming $1 + e^{2(-Vx^0+x^1)\sigma} - V > 0$. This assumption is needed so that the $\log|1+e^{2z^1\sigma}-V|$ term in Eq. (3.21) is well-behaved. An analogous procedure can be followed for the assumption $1+e^{2(-Vx^0+x^1)\sigma}-V<0$. This procedure can also be applied to find $w^0(x^0, x^1)$.

The first step is to make the substitution $X \equiv x^1 - V\,x^0$. This reduces $w^1(x^0, x^1)$ to a function of a single variable. The new expression is

$$\begin{aligned} w^1(x^0, x^1) =& \frac{-4X\sigma + V(1+V)\log\left(1+e^{2X\sigma}-V\right)}{4\left(-1+V^2\right)\sigma} \\ &+ \frac{(-1+V)V\log\left(1+e^{2X\sigma}+V\right)}{4\left(-1+V^2\right)\sigma}. \end{aligned} \tag{3.28}$$

The laws of logarithms are then used to simplify the equation. The result is

$$w^1(x^0, x^1) = \frac{-4X\sigma + \log\left(\left(1+e^{2X\sigma}-V\right)^{V(1+V)}\left(1+e^{2X\sigma}+V\right)^{(-1+V)V}\right)}{4\left(-1+V^2\right)\sigma}. \tag{3.29}$$

We make the substitution $p \equiv e^{2X\sigma}$ and simplify using properties of logarithms. This yields

$$w^1(x^0, x^1) = \frac{\log\left(\frac{(1+p-V)^{V(1+V)}(1+p+V)^{(-1+V)V}}{p^2}\right)}{4\left(-1+V^2\right)\sigma} \tag{3.30}$$

How do we interpret p? Referring to Fig. 3.1, the warp bubble boundary occurs at $f(y^1) = 1/2$. From Eq. (3.7), this corresponds to $\sigma\left(x^1 - V\,x^0\right) = 0$. Since this is the boundary of the warp bubble, we can now define "far-outside the warp bubble" to be the region where $x^1 - V\,x^0 \ll 0$ and "far-inside the warp bubble" to be $x^1 - V\,x^0 \gg 0$. So we have defined far-inside and far-outside the warp bubble in terms of $X \equiv x^1 - V\,x^0$. How does this fit together with the substitution $p \equiv e^{2X\sigma}$? If $p = 0$ then $X = -\infty$. Since $-\infty \ll 0$, this means that $p = 0$ corresponds to far-outside the warp bubble. Likewise, if $p = \infty$ then $X = \infty$. This means that $p = \infty$ corresponds to a position far-inside the warp bubble. Therefore, if we wish to find an approximate coordinate transformation for far-outside or far-inside the bubble, then we should expand Eq. (3.30) in a Taylor series about $p = 0$ or $p = \infty$. Here we will expand about $p = \infty$ to get the approximate coordinate transformation far-inside the warp bubble. To third order, the expansion yields

$$w^1(x^0, x^1) \approx \frac{V^2}{3\sigma p^3} - \frac{V^2}{4\sigma p^2} - \frac{\log\left(\frac{1}{p}\right)}{2\sigma}. \tag{3.31}$$

Upon substituting in the original variables, the approximate coordinate transformation is

$$w^1(x^0,\, x^1) \approx \frac{V^2 e^{-6\sigma(x^1 - Vx^0)}}{3\sigma} - \frac{V^2 e^{-4\sigma(x^1 - Vx^0)}}{4\sigma} - Vx^0 + x^1 \tag{3.32}$$

for far-inside the warp bubble. Following a similar procedure, approximate coordinate transformations can be found for w^0 for both far-inside and far-outside the bubble. For far-outside the warp bubble and $V < 1$ the transformation looks like

$$w^1(x^0,\, x^1) \approx \frac{\log\left((1-V)^{V(V+1)}(V+1)^{(V-1)V}\right) - 4\sigma(x^1 - Vx^0)}{4\sigma\left(V^2-1\right)} - \frac{V^2 e^{2\sigma(x^1 - Vx^0)}}{\sigma\left(V^2-1\right)^2} \tag{3.33}$$

$$\begin{aligned} w^0(x^0,\, x^1) \approx{}& \frac{V\left(\log\left((1-V)^{V+1}(V+1)^{1-V}\right) - 4\sigma(x^1 - Vx^0)\right)}{4\sigma\left(V^2-1\right)} \\ &- \frac{(1-V)^{-V}V(V+1)^{V-2}\left(V^2+1\right)\left(\frac{2}{V+1}-1\right)^V e^{2\sigma(x^1 - Vx^0)}}{2\sigma(V-1)^2}. \end{aligned} \tag{3.34}$$

For far-inside the warp bubble and $V < 1$ the transformation looks like

$$w^1(x^0,\, x^1) \approx -\frac{V^2 e^{-4\sigma(x^1 - Vx^0)}}{4\sigma} - Vx^0 + x^1 \tag{3.35}$$

$$w^0(x^0,\, x^1) \approx -\frac{V e^{-4\sigma(x^1 - Vx^0)}}{4\sigma} + \frac{V e^{-2\sigma(x^1 - Vx^0)}}{2\sigma} + x^0. \tag{3.36}$$

3.4 Results & Analysis

Using the coordinate transformations derived previously, it is now possible to describe wave propagation. The procedure is as follows:

1. Specify the shape of a wavepacket in x^α coordinates either far-inside or far-outside of the warp bubble. This is the initial condition.

2. Make the coordinate transformation from x^α coordinates to w^α coordinates using the appropriate transformation derived in Section 3.2.

3. Propagate the wave in w^α coordinates. This is done using the known solution of the wave equation in w^α coordinates: $\phi(w^0, w^1) = F(w^1 - w^0) + G(w^1 + w^0)$.

4. After propagating the wave, transform back from w^α coordinates to the original x^α coordinates using the approximate coordinate transformations derived in Section 3.3.

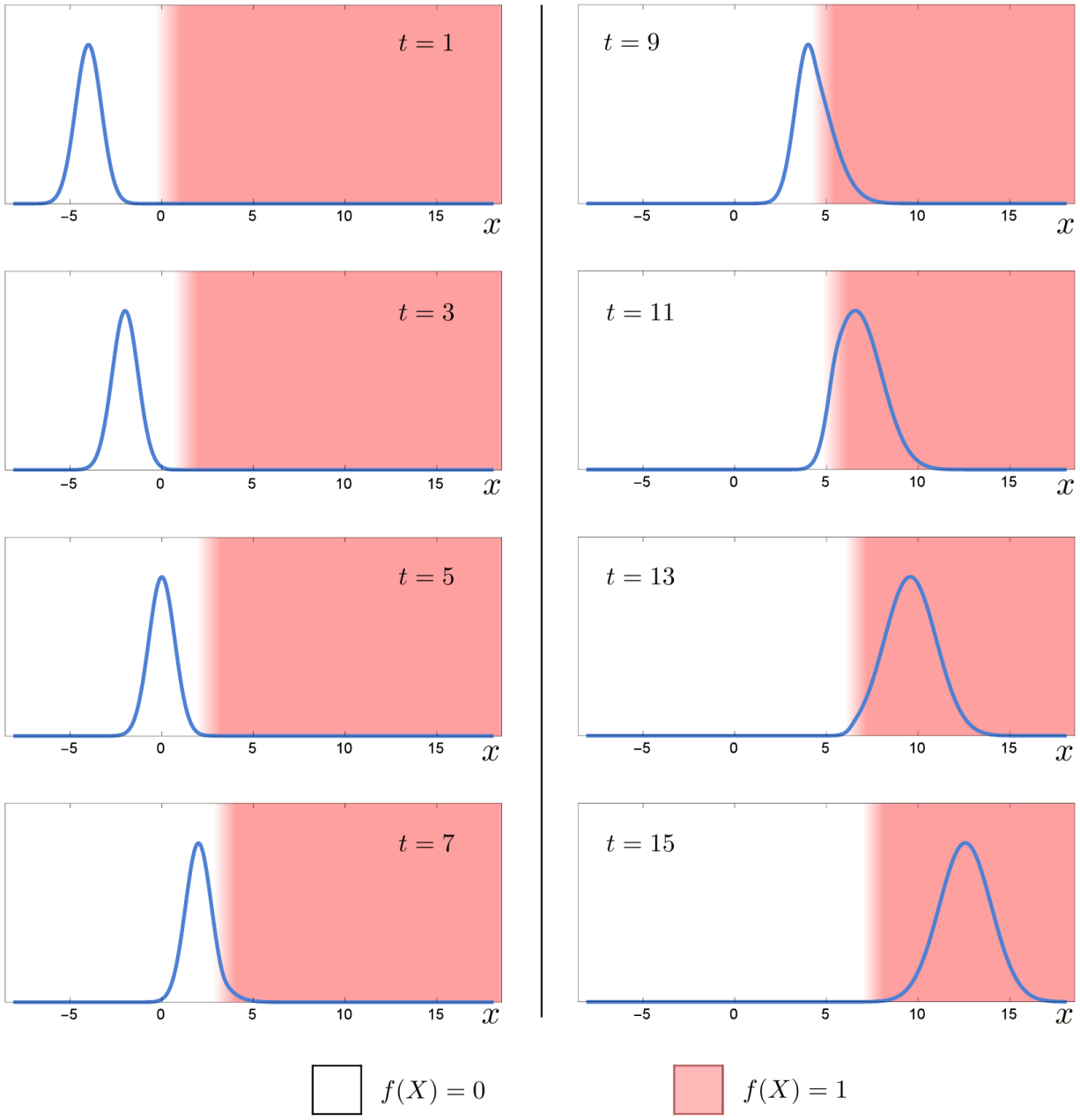

Figure 3.2: A wavepacket enters a warp drive with parameters $V = 0.5$, $\sigma = 5$. The white region represents flat spacetime. The pink region represents the inside of the warp bubble. The transition region between white and pink represents the boundary of the warp bubble and is governed by Eq. (3.7). The wavepacket undergoes an apparent expansion corresponding to a redshift. The apparent velocity of the wave also increases from $c = 1$ to $c = 1 + V = 1.5$.

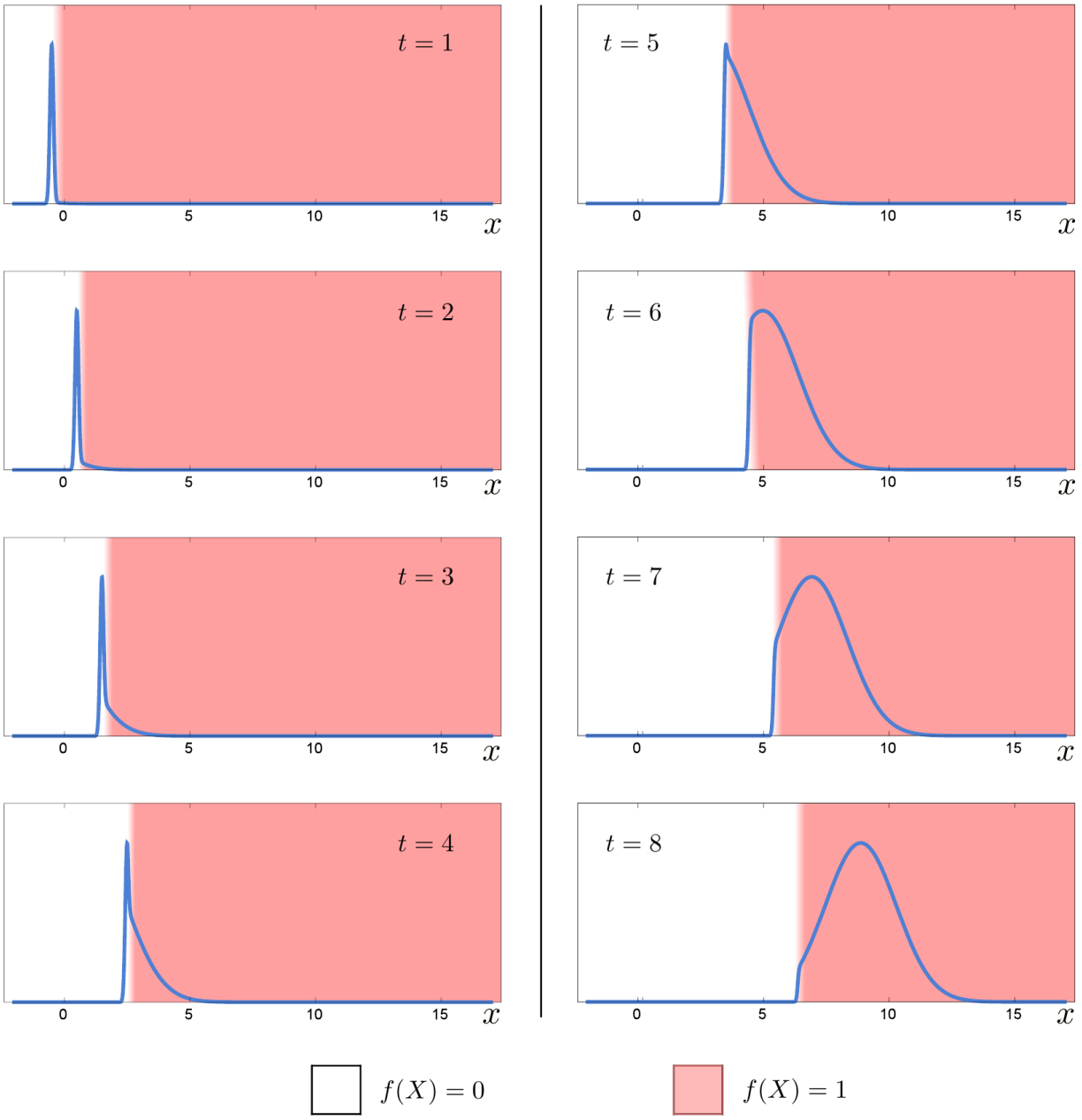

Figure 3.3: A wavepacket enters a warp drive with parameters $V = 0.95$, $\sigma = 20$. The wavepacket appears to rapidly expand as it enters the warp drive. This can be attributed to an increase in the apparent velocity of light in a warp drive: the part of the wave that has entered the warp bubble is suddenly boosted to an apparent velocity of $c = 1 + V = 1.95$ while the lagging part remains at $c = 1$ until it can "catch up". To an outside observer, it appears as if the wave has been redshifted.

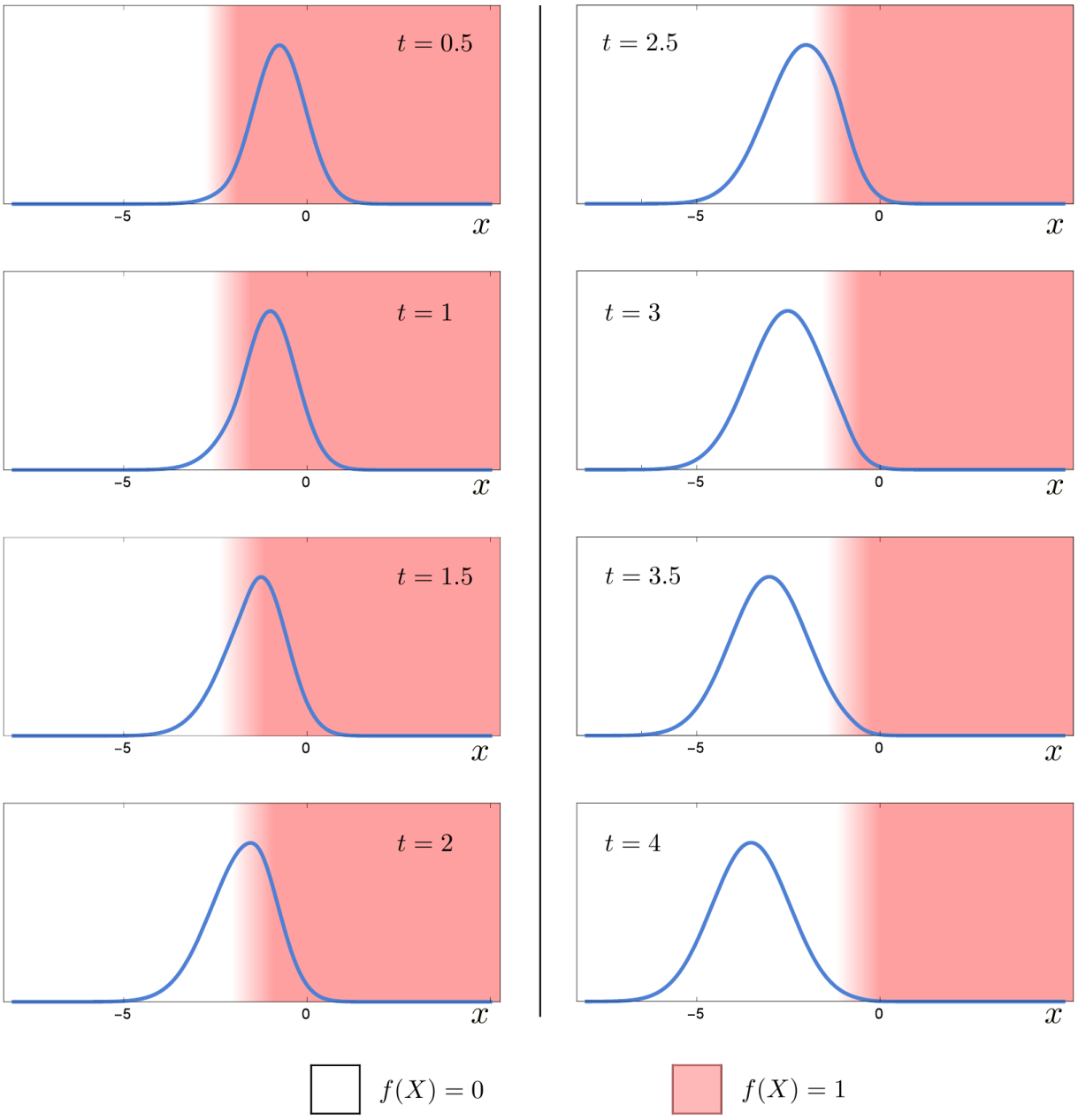

Figure 3.4: A wavepacket that is intially inside a $V = 0.5$, $\sigma = 5$ warp drive leaves from the left. In contrast to Fig. 3.2 and Fig. 3.3, the wavepacket and the warp drive are now moving in opposite directions. Since the warp drive is moving to the right and the wavepacket is moving to the left, the apparent velocity of the wavepacket is $c = -1 + V = -0.5$ in the pink region. Once it enters the white region, it appears to return to the usual velocity of c.

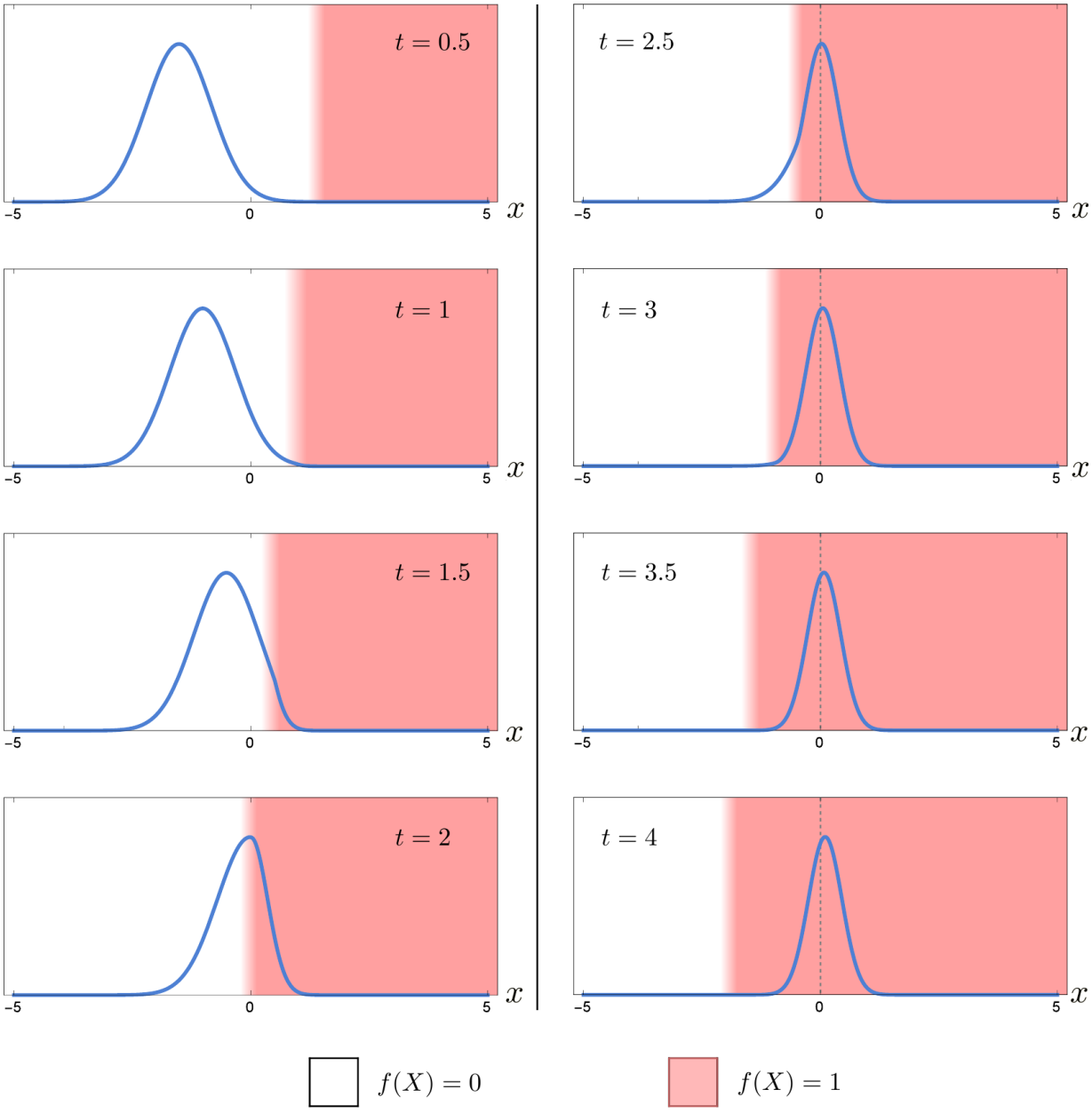

Figure 3.5: A wavepacket collides head-on with a $V = 0.95$, $\sigma = 20$ warp drive. The wavepacket undergoes a contraction after entering the warp bubble. This corresponds to an apparent blueshift. It is notable that the wavepacket appears to be almost motionless after entering the bubble. This is because the apparent velocity of the wavepacket is $c = 1 + (-0.95) = 0.05$ and so it appears to be moving at only 1/20th of the speed of light.

Some of the interesting scenarios are illustrated in Fig. 3.2, Fig. 3.3, Fig. 3.4, and Fig. 3.5. We start with a wavepacket inside or outside the warp drive. We then send it towards the warp bubble boundary.

3.4.1 Apparent Change in Light Velocity

In every case, it is found that the apparent velocity of the wavepacket changes when it crosses the boundary. It is found that the wavepacket always travels with a velocity $c = 1$ when it is outside the warp drive in Minkowski space. This is to be expected from the theory of special relativity. However, when the wavepacket is inside the warp bubble, it travels with a velocity $c = \pm 1 + V$. The $+1$ case corresponds to a right-moving wavepacket and the -1 case corresponds to a left-moving wavepacket. This is exactly what was predicted in Eq. (2.10). The best illustration of this effect is given in Fig. 3.5. A wavepacket and a $V = 0.95$ warp drive suffer a head-on collision. Before the collision, the wavepacket is in Minkowski space and has the expected velocity of $c = 1$. After the collision, the wavepacket is in the warp drive and has the apparent velocity $c = 1 + (-0.95) = 0.05$. This is only 1/20th of the regular speed of light and the wavepacket appears to be almost motionless.

3.4.2 Redshift & Blueshift

It is found that a wavepacket passing through the warp bubble boundary will undergo an expansion or contraction. For example, consider the situation that is illustrated in Fig. 3.3. An extremely narrow wavepacket enters a forward-moving warp drive from behind. As it passes through the warp bubble boundary, it undergoes a significant expansion. The explanation for this phenomenon is intuitive. Initially, the entire wavepacket is in Minkowski space and travels at a velocity $c = 1$. The front of the wavepacket soon enters the warp bubble. Once it is inside, the front of the wavepacket is forced to travel with a velocity given by Eq. (2.10). However, the back of the wavepacket is still in Minkowski space and so it is still traveling at a velocity $c = 1$. This difference in speed effectively "stretches out" the wavepacket until the back of the wavepacket reaches the warp bubble boundary.

The expansion and contraction of the wavepacket corresponds to an apparent redshift or blueshift of light. Physically, this would manifest itself as a change in the color of visible light as it passes through the warp bubble boundary. Clark et al. predicted this in their numerical study of null geodesics [23]. According to that analysis, the energy of a photon as measured by an observer in the warp bubble will be

$$E_{\mathrm{o}} = (1 \pm V)\, E_{\infty} \tag{3.37}$$

where E_{o} is the measurement of the photon energy by an observer inside the warp bubble and E_{∞} is a measurement by an outside observer. The $+V$ case in Eq. (3.37) corresponds to a photon

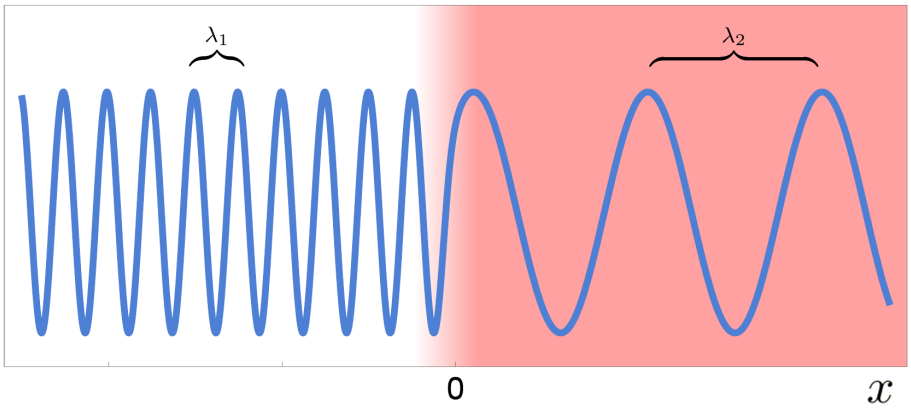

Figure 3.6: The redshift of light by a warp drive. A sinusoidal wave incident on a warp drive will undergo an expansion or contraction. The apparent redshift can be determined by comparing the relative wavelengths λ_1 and λ_2 of the light. According to Clark et al. [23], the redshift should be given by Eq. (3.37).

colliding with the warp drive head-on (as in Fig. 3.5) and the $-V$ case corresponds to a photon traveling in the same direction as the warp drive (as in Fig. 3.2). We can confirm Clark's result in Eq. (3.37) by propagating an infinite sinusoidal wave through the warp bubble boundary. This situation is depicted in Fig. 3.6.

The values of λ_1 and λ_2 in our analysis can be computed numerically. Using the relation $E = hc/\lambda$, it is found that the calculated redshift is in excellent agreement with Eq. (3.37) predicted by Clark. This provides an extra confirmation for our method and results.

3.4.3 Apparent Horizon Formation for $V > 1$

All the physics in this section so far has been for warp drives with speeds $V < 1$. It would be very interesting to study wave propagation for faster-than-light warp drives. Unfortunately, complications arise when $V \geq 1$ is considered. This is because the transformations of Eq. (3.21) and Eq. (3.27) contain a term of the form $|1 + e^{2z^1\sigma} - V|$. This requires a case distinction:

$$|1 + e^{2z^1\sigma} - V| = \begin{cases} 1 + e^{2z^1\sigma} - V, & V < 1 + e^{2z^1\sigma} \\ -(1 + e^{2z^1\sigma} - V), & V > 1 + e^{2z^1\sigma} \end{cases}. \tag{3.38}$$

The switch between the two cases will occur when

$$z^1 = \frac{\log(-1 + V)}{2\sigma}. \tag{3.39}$$

This means we have two different forms of $q(z^1)$ depending on the value of V and both will diagonalize the matrix of Eq. (3.13). Ultimately, this means that we will have to define two

separate functions for $w^1(x^0, x^1)$ according to the case distinction. First, for the case where $1 + e^{2z^1\sigma} - V < 0$, we define

$$\begin{aligned} w^1_-(x^0,\, x^1) = \frac{-Vx^0 + x^1}{-1+V^2} - \frac{V\log\left(-1 - e^{2(-Vx^0+x^1)\sigma} + V\right)}{4(-1+V)\sigma} \\ - \frac{V\log\left(1 + e^{2(-Vx^0+x^1)\sigma} + V\right)}{4(1+V)\sigma}. \end{aligned} \tag{3.40}$$

Secondly, for the case where $1 + e^{2z^1\sigma} - V > 0$, we define

$$\begin{aligned} w^1_+(x^0,\, x^1) = \frac{Vx^0 - x^1}{-1+V^2} + \frac{V\log\left(1 + e^{2(-Vx^0+x^1)\sigma} - V\right)}{4(-1+V)\sigma} \\ + \frac{V\log\left(1 + e^{2(-Vx^0+x^1)\sigma} + V\right)}{4(1+V)\sigma}. \end{aligned} \tag{3.41}$$

We will also need to define two functions for $w^0(x^0, x^1)$ according to the case distinction given in Eq. (3.38):

$$\begin{aligned} w^0_+(x^0,\, x^1) = x^0 + \frac{V\left(-Vx^0 + x^1\right)}{-1+V^2} \\ + \frac{V(-1+V)\log\left(1 + e^{2(-Vx^0+x^1)\sigma} + V\right)}{4\sigma\left(-1+V^2\right)} \\ - \frac{V(1+V)\log\left(1 + e^{2(-Vx^0+x^1)\sigma} - V\right)}{4\sigma\left(-1+V^2\right)} \end{aligned} \tag{3.42}$$

$$\begin{aligned} w^0_-(x^0,\, x^1) = x^0 + \frac{V\left(-Vx^0 + x^1\right)}{-1+V^2} \\ + \frac{V(-1+V)\log\left(1 + e^{2(-Vx^0+x^1)\sigma} + V\right)}{4\sigma\left(-1+V^2\right)} \\ - \frac{V(1+V)\log\left(-1 - e^{2(-Vx^0+x^1)\sigma} + V\right)}{4\sigma\left(-1+V^2\right)}. \end{aligned} \tag{3.43}$$

When $V < 1$, $|1 + e^{2z^1\sigma} - V| = 1 + e^{2z^1\sigma} - V$ and the coordinate transformations are continuous everywhere. This is shown in Fig. 3.7 for various V. However, when $V > 1$, a coordinate singularity appears in $w^1(x^0, x^1)$ and $w^0(x^0, x^1)$. This is shown in Fig. 3.8. This prevents us from having an exact description of light propagation for the case of $V > 1$. This is precisely why the results presented in Fig. 3.2, Fig. 3.3, Fig. 3.4, and Fig. 3.5 were all for the case of $V < 1$.

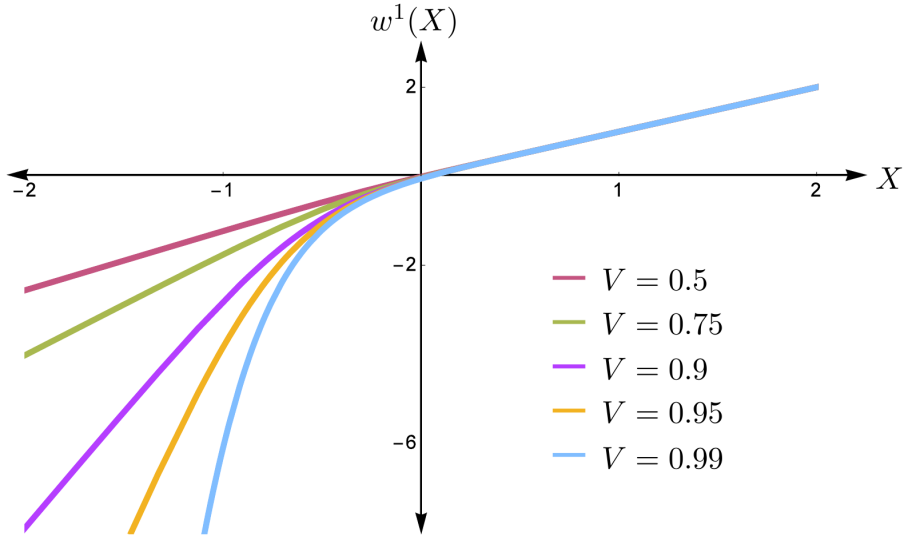

Figure 3.7: The coordinate transformations $w^1(x^0, x^1)$ is continuous everywhere when $V < 1$. Plotted is $w^1(X)$ for a variety of V and $\sigma = 2$. When V is small, the coordinate transformation between x^α and w^α is approximately linear. As V increases, a "kink" appears to form. Although it is not plotted here, $w^0(x^0, x^1)$ is likewise continuous.

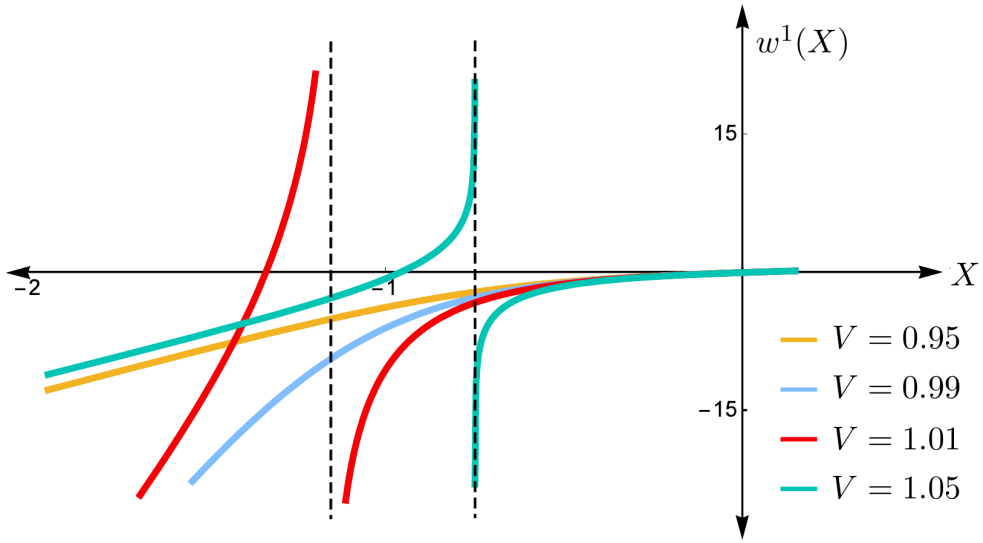

Figure 3.8: The coordinate transformations $w^1(x^0, x^1)$ is discontinuous when $V > 1$. Plotted is $w^1(X)$ for a variety of V and $\sigma = 2$. This plot shows how the asymptote forms as V passes from $V < 1$ to $V > 1$. Although it is not plotted here, $w^0(x^0, x^1)$ is likewise discontinuous for $V > 1$. Since the coordinate transformations are discontinuous, we cannot describe light propagation for the case of $V > 1$.

As can be seen from Fig. 3.8, the singularity forms at $V = 1$ and moves to the right as V increases. This may correspond to an *apparent horizon*. In the words of Rindler, a horizon is a "a frontier between things observable and things unobservable" [21]. It is a boundary beyond which events are unobservable. In the context of the Alcubierre metric, the presence of this horizon makes sense. A light ray trying to catch up with a faster-than-light warp drive will never be able to reach it. Where will the horizon form? Using a method from [35], we can determine the location. The two-dimensional Alcubierre metric of Eq. (3.6) can be rewritten as

$$ds^2 = -(1 - V^2 f(x - V\,t)^2)\,dt^2 - 2V\,f(x - V\,t)\,dt\,dx + dx^2. \tag{3.44}$$

Upon making the substitution $x = y + V\,t$, the metric becomes

$$ds^2 = -(1 - V^2\,(1 - f(y))^2)\left(dt - \frac{V(1 - f(y))}{1 - V^2\,(1 - f(y))^2}dy\right)^2 + \frac{dy^2}{1 - V^2\,(1 - f(y))^2} \tag{3.45}$$

This metric is valid for all $y > 0$ provided that $V < 1$. However, setting $V > 1$ will result in a singularity at the location where $1 - V^2\,(1 - f(y))^2 = 0$. This corresponds to the location where

$$f(y) = 1 - \frac{1}{V}. \tag{3.46}$$

For the cases where $V < 1$, there is no horizon because $f(y) \geq 0$ everywhere. If we choose the particular shaping function of Eq. (4.48), the horizon forms at

$$\frac{1}{2}(\tanh(\sigma y) + 1) = 1 - \frac{1}{V} \tag{3.47}$$

or equivalently

$$y = \frac{1}{\sigma}\,\operatorname{arctanh}\left(1 - \frac{2}{V}\right). \tag{3.48}$$

This apparent horizon of the Alcubierre metric will be studied in greater detail in Chapter 4.

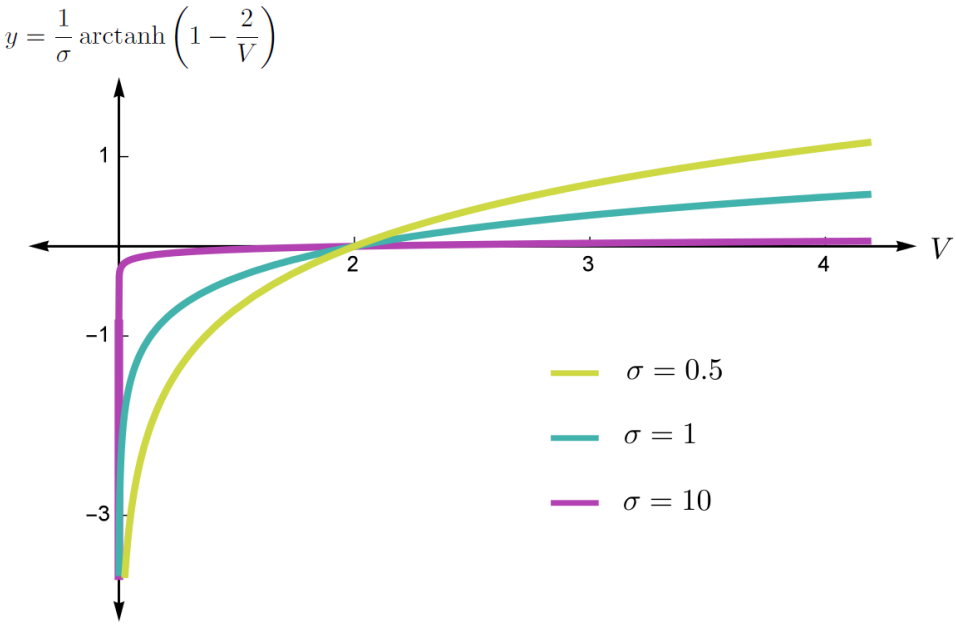

Figure 3.9: The location of the apparent horizon in the Alcubierre metric for various σ. Eq. (3.48) dictates that the horizon will form $y = -\infty$ for $V = 1$. For $V > 1$, it will move to finite values of y. This is in agreement with the rightward shifting of the asymptote in Fig. 3.8.

Chapter 4

Conformal Light-Cone Coordinates

The methods of Chapter 3 provided an analytic description of light propagation in a $V < 1$ warp drive. In this chapter, we present a second method for describing the propagation of light in the Alcubierre metric. This method permits us to describe wave propagation for accelerating warp drives and the $V > 1$ case. It also provides new insights into the formation of an apparent horizon in the Alcubierre metric.

4.1 Overview of Light-Cone Coordinates

Light-cone coordinates is a system of coordinates that is commonly used in special relativity. The basic idea is to define two coordinates x_+ and x_- that correspond to the trajectories of light rays. In two dimensions, these coordinates are taken to be a linear combination of the time coordinate t and the spatial coordinate x:

$$x_+ = \frac{1}{\sqrt{2}}(x + t) \tag{4.1}$$

$$x_- = \frac{1}{\sqrt{2}}(x - t). \tag{4.2}$$

In this coordinate system, the worldlines of light rays emitted from the origin correspond to the coordinate axes. In other words, the x_+ and x_- axes make a 45° angle with the x and t axes of the original coordinate system.

This new coordinate system will give a different form for the Minkowski metric. In terms of light-cone coordinates, the metric looks like

$$ds^2 = 2\, dx_+\, dx_-. \tag{4.3}$$

The wave equation will also look different in light-cone coordinates. The standard wave equation

$$\left(\partial_x^2 - \partial_t^2\right)\, \phi(x,t) = 0 \tag{4.4}$$

becomes

$$\partial_{x_+}\partial_{x_-}\, \phi(x_+, x_-) = 0. \tag{4.5}$$

Although the metric tensor and the wave equation look different in light-cone coordinates, they

still describe the exact same physics. The only difference is a new coordinate system.

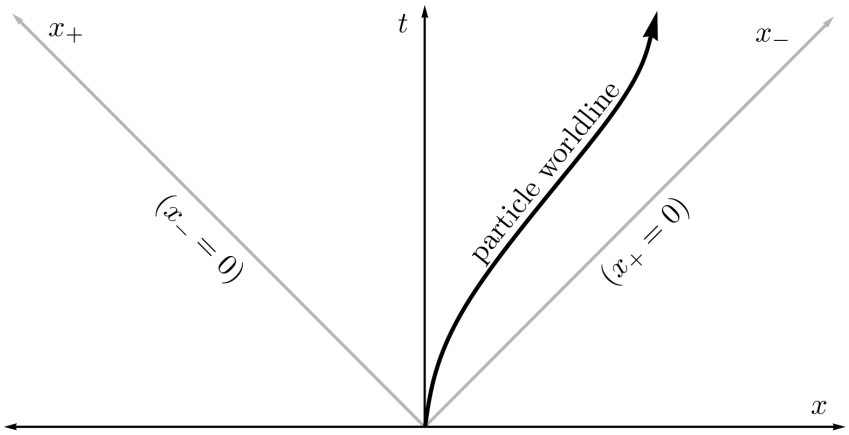

Figure 4.1: A spacetime diagram with the light-cone coordinate system. The trajectories of light rays ($x = \pm t$) become the new coordinate axes (x_- and x_+). The coordinate axes of x_- and x_+ make a 45° angle with the standard x-t coordinate system.

The idea of light-cone coordinates can be generalized for curved spacetimes. In Section 3.1, we learned that every two-dimensional metric can be reduced through a coordinate transformation to the Minkowski metric multiplied by a factor Ω^2:

$$ds^2 = \Omega^2 \left(-dT^2 + dX^2\right). \tag{4.6}$$

For a metric of this form, we can define a set of coordinates that are analogous to light-cone coordinates. These coordinates are known as *conformal light-cone coordinates*. In these new coordinates, the metric has the form

$$ds^2 = 2\,\Omega^2\, dx_+\, dx_- \tag{4.7}$$

and the wave equation is of the form

$$0 = \Omega^2\, \partial_{x_+} \partial_{x_-} \phi(x_+, x_-) \tag{4.8}$$

with general solutions given by

$$\phi(x_+, x_-) = \phi_+(x_+) + \phi_-(x_-). \tag{4.9}$$

It is very useful to express a metric in conformal light-cone coordinates because then the solution to the wave equation is very simple: it is just Eq. (4.9). This is useful for our purposes because the previous approach (Chapter 3) only provided solutions for the case $V < 1$. Expressing the

Alcubierre metric in conformal light-cone coordinates could extend our analysis to more general cases of wave propagation.

4.2 Light-Cone Coordinates for the Alcubierre Metric

The goal is find a coordinate transformation that will reduce the two-dimensional Alcubierre metric to conformal light-cone coordinates. The two-dimensional Alcubierre metric has the form

$$ds^2 = -dt^2 + (dx - \dot{x}_o f(x - x_o)dt)^2. \tag{4.10}$$

In this notation, the trajectory of an object at the center of the warp drive is given by $x_o = x_o(t)$. The velocity associated with this trajectory is $V(t) \equiv dx_o(t)/dt = \dot{x}_o$. This is also the velocity of the warp drive. Expanding out the line element yields

$$ds^2 = -dt^2 + dx^2 - 2\,\dot{x}_o\,f(x - x_o)\,dx\,dt + \dot{x}_o^2\,f(x - x_o)^2\,dt^2 \tag{4.11}$$

$$= (dx - \dot{x}_o f(x - x_o)dt - dt)(dx - \dot{x}_o f(x - x_o)dt + dt). \tag{4.12}$$

This expression can be simplified by making a change of variables $y = x - x_o(t)$. With this transformation, the metric can be written

$$ds^2 = -dt^2 + (dy - \dot{x}_o(f(y) - 1)dt - dt)^2 \tag{4.13}$$

$$= (dy - \dot{x}_o(f(y) - 1)dt - dt)(dy - \dot{x}_o(f(y) - 1)dt + dt). \tag{4.14}$$

It is interesting that the line element of Eq. (4.14) has a "product structure" in that it is a product of two terms: $(dy - \dot{x}_o(f(y) - 1)dt \pm dt)$. This is a similar to the "product structure" of Eq. (4.3) for the metric in light-cone coordinates. With this similarity in mind, appropriate light-cone coordinates for the Alcubierre metric could be

$$dx_\pm = \alpha_\pm(t, y)(dy - \dot{x}_o(f(y) - 1)dt \pm dt). \tag{4.15}$$

The term $\alpha_\pm(t, y)$ represents two unknown functions. To determine the $\alpha_\pm(t, y)$ functions, we can expand the previous equation to get

$$dx_\pm = \alpha_\pm(t, y)\,dy - \alpha_\pm(t, y)\,\dot{x}_o(f(y) - 1)dt \pm \alpha_\pm(t, y)\,dt. \tag{4.16}$$

We can compare Eq. (4.16) to the relation

$$dx_\pm = \frac{\partial x_\pm}{\partial t}dt + \frac{\partial x_\pm}{\partial y}dy \tag{4.17}$$

to determine two expressions for the derivatives of the light-cone coordinates. These derivatives are given by

$$\frac{\partial x_\pm}{\partial y} = \alpha_\pm(t, y) \tag{4.18}$$

$$\frac{\partial x_\pm}{\partial t} = \alpha_\pm(t, y)\,(\pm 1 - \dot{x}_0(f(y) - 1)). \tag{4.19}$$

Substituting Eq. (4.18) into Eq. (4.19) yields

$$\frac{\partial x_\pm}{\partial t} = (\pm 1 - \dot{x}_\mathrm{o}(f(y) - 1))\,\frac{\partial x_\pm}{\partial y}. \tag{4.20}$$

This partial differential equation can be solved using the *method of characteristics* [36]. The idea behind the method is to define curves along which the partial differential equation can be reduced to an ordinary differential equation. Once the solution to the ordinary differential equation is found along the curves, it can be transformed into the solution of the original partial differential equation. To begin, we introduce a two-dimensional vector

$$\vec{T} = (1,\, \mp 1 + \dot{x}_\mathrm{o}(f(y) - 1)). \tag{4.21}$$

With this vector, Eq. (4.20) can be rewritten as $\vec{T}\cdot\nabla x_\pm = 0$ where $\nabla = (\partial_t, \partial_y)$. This implies that $x_\pm$ remains constant along curves for which $\vec{T}$ is a tangent vector. If the curve is parametrized by s as $(t(s), y(s))$ then

$$0 = \frac{d}{ds} x_\pm(t(s), y(s)) \tag{4.22}$$

$$= \frac{dt}{ds}\frac{\partial}{\partial t} x_\pm + \frac{dy}{ds}\frac{\partial}{\partial y} x_\pm. \tag{4.23}$$

This is equivalent to

$$\left(\frac{dt}{ds}, \frac{dy}{ds}\right) \cdot \nabla x_\pm = 0 \tag{4.24}$$

which implies that $\vec{T}$ should be chosen as $\vec{T} = (\frac{dt}{ds}, \frac{dy}{ds})$. With this choice, the system of differential equations becomes

$$\frac{dt}{ds} = 1 \tag{4.25}$$

$$\frac{dy}{ds} = \mp 1 + \dot{x}_\mathrm{o}(f(y) - 1). \tag{4.26}$$

This can be simplified by setting $t = s$:

$$\frac{dy}{dt} = \mp 1 + \dot{x}_{\rm o}(f(y) - 1). \tag{4.27}$$

The solution of Eq. (4.27) will yield the characteristic curves of Eq. (4.20). Once we have found the characteristic curves, we can construct the solution to Eq. (4.20) by forming a surface that is the union of the characteristic curves. This will yield the functional form of the light-cone coordinates for the Alcubierre metric.

4.2.1 Solution for Constant Velocity

We seek to solve Eq. (4.27). The simplest case is for $\dot{x}_{\rm o} = V = \text{constant}$. We start by rearranging Eq. (4.27) and integrating:

$$\int_{y_i}^{y} \frac{dy'}{\mp 1 + V(f(y') - 1)} = \int_{t_i}^{t} dt'. \tag{4.28}$$

This yields the relation

$$G_{\pm}(y) - G_{\pm}(y_i) = t - t_i \tag{4.29}$$

where we have defined

$$G_{\pm}(y) \equiv \int_{0}^{y} \frac{du}{\mp 1 + V(f(u) - 1)}. \tag{4.30}$$

Rearranging Eq. (4.29) yields

$$t_i - G_{\pm}(y_i) = t - G_{\pm}(y) \;=\; \text{constant} \tag{4.31}$$

which are characteristic curves of the solution. This implies that $x_{\pm}(t, y) = x_{\pm}(t_i, y_i) = \text{constant}$ along these lines and so the general solution is given by

$$x_{\pm}(t, x) = x_{\pm}(t - G_{\pm}(y)). \tag{4.32}$$

This is equivalent to

$$x_{+} = \frac{1}{\sqrt{2}}(t - G_{+}(y)) \tag{4.33}$$

$$x_{-} = -\frac{1}{\sqrt{2}}(t - G_{-}(y)) \tag{4.34}$$

which define the light-cone coordinates for the Alcubierre metric with constant V. It is notable that for the case of $V = 0$,

$$G_{\pm}(y) = \int_0^y \frac{du}{\mp 1} = \mp y = \mp x. \tag{4.35}$$

This implies that Eq. (4.33) and Eq. (4.34) will reduce to the light-cone coordinates for Minkowski space (Eq. (4.1) and Eq. (4.2)) when $V = 0$. Is this result reasonable? Yes, because the Alcubierre metric with $V = 0$ is equivalent to the Minkowski metric.

For constant V, it can be shown that Eq. (4.33) and Eq. (4.34) solve Eq. (4.20):

$$\frac{\partial x_{\pm}}{\partial t} = \pm\frac{1}{\sqrt{2}}\frac{\partial}{\partial t}(t - G_{\pm}(y)) = \pm\frac{1}{\sqrt{2}} \tag{4.36}$$

$$\begin{aligned}\frac{\partial x_{\pm}}{\partial y} &= \pm\frac{1}{\sqrt{2}}\frac{\partial}{\partial y}(t - G_{\pm}(y)) = \mp\frac{1}{\sqrt{2}}\frac{\partial}{\partial y}G_{\pm}(y) \\ &= \mp\frac{1}{\sqrt{2}}\frac{\partial}{\partial y}\int_0^y \frac{du}{\mp 1 + V(f(u) - 1)} \\ &= \mp\frac{1}{\sqrt{2}}\frac{1}{\mp 1 + V(f(y) - 1)}.\end{aligned} \tag{4.37}$$

When these derivatives are plugged in to Eq. (4.20), the differential equation will be satisfied.

It is now possible to find the solution to the wave equation in x-t coordinates. For simplicity, it is assumed that the solution consists solely of a right-moving wave. This means that x_+ remains constant during propagation and the solution depends on x_- only. The initial condition is taken to be

$$\phi(t = 0, x = 0) = \phi_i(t_i, x_i). \tag{4.38}$$

We assume $x_{\mathrm{o}}(t_i) = x_{\mathrm{o}}(0) = 0$. In other words, the warp drive starts at the origin at $t = 0$. Since $y = x - x_{\mathrm{o}}(t)$, it follows that

$$\begin{aligned}y(0) &= x(0) - x_{\mathrm{o}}(0) \\ &= x(0).\end{aligned} \tag{4.39}$$

We define $y_i = y(0)$ and $x_i = x(0)$ so that $y_i = x_i$. Invoking Eq. (4.31), we find

$$\begin{aligned}t_i - G_-(y_i) &= -G_-(x_i) \\ &= t - G_-(y).\end{aligned} \tag{4.40}$$

Solving for x_i, we determine

$$x_i = G_-^{-1}\left(G_-(y) - t\right). \tag{4.41}$$

The solution to the wave equation in x-t coordinates is then found to be

$$\begin{aligned}\phi(x,t) &= \phi_i(x_i) \\ &= \phi_i(G_-^{-1}(G_-(x-Vt)-t)).\end{aligned} \tag{4.42}$$

This provides an analytic description of wavepacket propagation. This solution depends only on V and the choice of $f(y)$ (since $f(y)$ determines $G_\pm(y)$ by Eq. (4.30)).

4.2.2 Solution for Arbitrary Velocity and Piecewise Linear $f(y)$

In this section, we consider a piecewise-defined shaping function to facilitate the study of the horizon. The shaping function is taken to be

$$f(y) = \begin{cases} 0, & \sigma y < -1 \\ \frac{1}{2}(1+\sigma y), & |\sigma y| \leq \frac{1}{2} \\ 1, & \sigma y > 1 \end{cases} \tag{4.43}$$

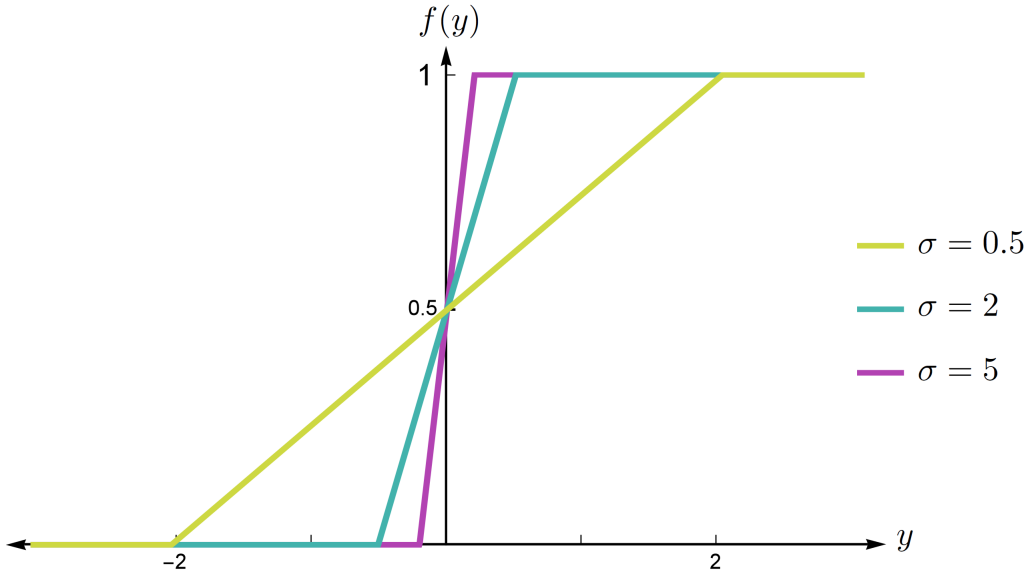

Figure 4.2: The piecewise linear shaping function of Eq. (4.43) for various σ. Note that this function is not twice differentiable and so it is not a completely valid shaping function. However, it serves as a good model for analyzing the horizon of the Alcubierre metric.

Note that the second derivative of Eq. (4.43) does not exist at all points and so it is not completely valid. Certain quantities (such as spacetime curvature) require the second derivative of the shaping function to exist but this is not satisfied here. However, this model will still provide value for analyzing the horizon.

For this choice of shaping function, Eq. (4.27) takes the form

$$\frac{dy}{dt} = \begin{cases} \mp 1 - \dot{x}_{\rm o}, & \sigma y < -1 \\ \mp 1 + \frac{\dot{x}_{\rm o}}{2}(\sigma y - 1), & |\sigma y| \leq \frac{1}{2} \\ \mp 1, & \sigma y > 1 \end{cases} \tag{4.44}$$

with solutions

$$y(t) = \begin{cases} \mp t - x_{\rm o}(t) + y_0 \pm t_0 + x_{\rm o}(0), & \sigma y < -1 \\ \frac{1}{\sigma}\left(1 - e^{\frac{\sigma}{2}(x_{\rm o}(t) - x_{\rm o}(t_1))}\right) + y_1 e^{\frac{\sigma}{2}(x_{\rm o}(t) - x_{\rm o}(t_1))} \mp \int_{t_1}^{t} dt' e^{\frac{\sigma}{2}(x_{\rm o}(t) - x_{\rm o}(t'))}, & |\sigma y| \leq \frac{1}{2} \\ \mp t \pm t_2 + y_2, & \sigma y > 1 \end{cases} \tag{4.45}$$

The times t_1 and t_2 are determined so that $\sigma y_1 = \sigma y(t_1) = -1$ and $\sigma y_2 = \sigma y(t_2) = 1$. This implies $y_1 = -1/\sigma$ and $y_2 = 1/\sigma$. This allows for the solution to be simplified to

$$y(t) = \begin{cases} \mp t - x_{\rm o}(t) + y_0 \pm t_0 + x_{\rm o}(0), & \sigma y < -1 \\ \frac{1}{\sigma}\left(1 - 2e^{\frac{\sigma}{2}(x_{\rm o}(t) - x_{\rm o}(t_1))}\right) \mp \int_{t_1}^{t} dt' e^{\frac{\sigma}{2}(x_{\rm o}(t) - x_{\rm o}(t'))}, & |\sigma y| \leq \frac{1}{2} \\ \mp t \pm t_2 + \frac{1}{\sigma}, & \sigma y > 1 \end{cases} \tag{4.46}$$

This solution will be valuable for analyzing the formation of the horizon.

4.2.3 Solution for Linear Acceleration, $y < 0$ to Analyze Horizon Formation

From Fig. 3.9, the horizon remains in the region $y < 0$ as long as $V < 2$. We can exploit this fact to find an approximate description of horizon formation as long as $V < 2$. We consider the case of a linearly accelerating warp drive,

$$x_{\rm o}(t) = \frac{1}{2}at^2, \tag{4.47}$$

and the shaping function given by

$$f(y) = \frac{1}{2}(\tanh(\sigma y) + 1). \tag{4.48}$$

Eq. (4.27) then takes the form

$$\frac{dy}{dt} = \mp 1 - \frac{at}{1 + e^{2\sigma y}}. \tag{4.49}$$

If we can anticipate that the horizon will form for $y < 0$ and $|y| \gg \frac{1}{\sigma}$, we can make the approximation

$$\frac{1}{1 + e^{2\sigma y}} \approx 1 - e^{2\sigma y}. \tag{4.50}$$

This yields

$$\frac{dy}{dt} = \mp 1 - at + ate^{2\sigma y}. \tag{4.51}$$

This approximation is equivalent to setting $f(y) = e^{2\sigma y}$. Since we are working in the region $y < -\frac{1}{\sigma}$, we can look to the solution found in Eq. (4.46). Making the ansatz $y(t) = \mp t - \frac{1}{2}at^2 + u(t)$ yields the result

$$\dot{u}\, e^{-2\sigma u} = -ae^{\mp 2\sigma t - \sigma a t^2}. \tag{4.52}$$

This equation can be integrated to yield

$$e^{-2\sigma u(t)} = -1 + e^{-2\sigma y_0} + e^{\mp 2\sigma t - a\sigma t^2} + \sqrt{\frac{\pi\sigma}{a}} e^{\frac{\sigma}{a}} \left[\operatorname{erf}\left(\sqrt{\frac{\sigma}{a}}(1 \pm at) \right) - \operatorname{erf}\left(\sqrt{\frac{\sigma}{a}} \right) \right], \tag{4.53}$$

where $\operatorname{erf}(x)$ is the error function:

$$\operatorname{erf}(x) = \frac{1}{\sqrt{\pi}} \int_{-x}^{x} e^{-t^2}\, dt. \tag{4.54}$$

Eq. (4.53) is the solution to Eq. (4.51) and enables us to find a relation between t and y. This relationship will specify the correct characteristic lines. From the characteristic lines, it will be possible to construct the proper light-cone coordinates. The characteristic lines are given by

$$\text{constant} = -1 + e^{-2\sigma y_0} \tag{4.55}$$

$$= (e^{-2\sigma y} - 1)e^{\mp 2\sigma t - a\sigma t^2} - \sqrt{\frac{\pi\sigma}{a}} e^{\frac{\sigma}{a}} \left[\operatorname{erf}\left(\sqrt{\frac{\sigma}{a}}(1 \pm at) \right) - \operatorname{erf}\left(\sqrt{\frac{\sigma}{a}} \right) \right]. \tag{4.56}$$

This implies that the light-cone coordinates are given by

$$\tilde{x}_{\pm} = (e^{-2\sigma y} - 1)e^{\mp 2\sigma t - a\sigma t^2} - \sqrt{\frac{\pi\sigma}{a}} e^{\frac{\sigma}{a}} \left[\operatorname{erf}\left(\sqrt{\frac{\sigma}{a}}(1 \pm at) \right) - \operatorname{erf}\left(\sqrt{\frac{\sigma}{a}} \right) \right]. \tag{4.57}$$

If $a = 0$, the velocity of the object will be $V(t) = x_{\mathrm{o}}(t) = \frac{1}{2}(0)t^2 = 0$. We would then expect the Alcubierre metric to be identical to the Minkowski metric and the light-cone coordinates to reduce to Eq. (4.1) and Eq. (4.2). Taking the limit of $\tilde{x}_{\pm}$ yields

$$\lim_{a \to 0} \tilde{x}_{\pm} = -1 + e^{\pm 2(t+y)\sigma} \tag{4.58}$$

We therefore redefine the light-cone coordinates as

$$x_{\pm} = -\frac{1}{2\sqrt{2}\,\sigma} \ln(1 + \tilde{x}_{\pm}). \tag{4.59}$$

To show that this is equivalent to Eq. (4.1) and Eq. (4.2) for $V = 0$, we take the asymptotic expansion of the error function for real x and $|x| \gg 1$:

$$\operatorname{erf}(x) \approx 1 - \frac{e^{-x^2}}{x\sqrt{\pi}}, \tag{4.60}$$

When this approximation is made, $x_\pm$ reduces to

$$x_+ = \frac{1}{\sqrt{2}}(y + t) \tag{4.61}$$

$$x_- = \frac{1}{\sqrt{2}}(y - t) \tag{4.62}$$

If $V = 0$, then $y = x$ and we get the flat space light-cone coordinates of Eq. (4.1) and Eq. (4.2).

Now that we have an explicit form for the light-cone coordinates, we can construct the solution to the wave equation. The solution is the sum of left and right moving waves: $g_+(x_+) + g_-(x_-)$. As we did in Section 4.2.1, we can construct the general solution in the standard way:

$$g_\pm(x_\pm) = g_\pm\left(-\frac{1}{2\sqrt{2\sigma}}\ln(1 + \tilde{x}_\pm)\right). \tag{4.63}$$

4.3 Results & Analysis

Conformal light-cone coordinates provide a convenient method for calculating the trajectories of light rays on a spacetime diagram of the Alcubierre metric. To find these trajectories, we start with Eq. (4.27). The substitution $y = x - x_o(t)$ results in

$$\frac{dy}{dt} = \frac{dx}{dt} - \frac{dx_o}{dt} = \mp 1 + \dot{x}_o(f(y) - 1) = \mp 1 + \dot{x}_o\, f(y) - \dot{x}_o. \tag{4.64}$$

Since $\frac{dx_o}{dt} = \dot{x}_o$, the terms cancel out on both sides of the equation. We are left with the equation for the light cones in the Alcubierre metric:

$$\frac{dx}{dt} = \mp 1 + \dot{x}_o\, f(y) \tag{4.65}$$

The -1 case determines the trajectories of left-moving (x_+) rays and the $+1$ case determines the trajectories of right-moving (x_-) rays. The plotted trajectories are shown in Fig. 4.3 and 4.4. In Minkowski space, the rays travel along lines of $x = \pm t$. However, rays become "tilted" inside the warp drive. To an outside observer, right-moving waves appear to be going faster than c and left-moving waves appear to be going slower than c. This result agrees with the previous findings of this thesis (in particular, Fig. 3.2, Fig. 3.3, Fig. 3.4, and Fig. 3.5).

Conformal light-cone coordinates also permit the analysis of light propagation in a $V =$ constant warp drive, as in Chapter 3. In Section 4.2.1, we found that the solution to the wave

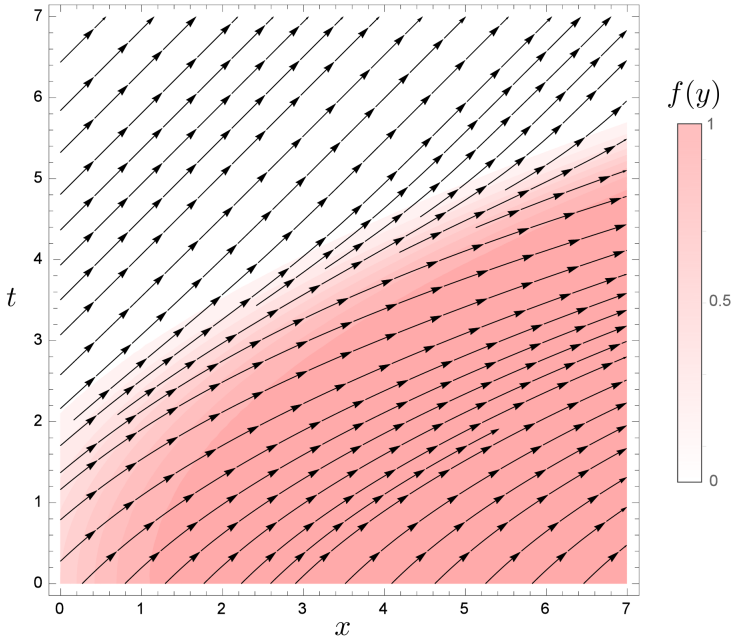

Figure 4.3: A spacetime diagram of right-moving (x_-) light rays for the Alcubierre metric. Here, a warp drive starts at rest and accelerates linearly. The trajectory is given by $x_o(t) = \frac{1}{2}a\,t^2$ with $a = 0.5$. The shaping function is taken to be Eq. (4.48) with $\sigma = 1$. The pink shaded region represents the inside of the warp drive and the white region is Minkowski space. When inside the warp drive, the light rays appear to be traveling faster than they do in Minkowski space.

equation for constant V is given by Eq. (4.42). To analyze this solution, we take the shaping function to be given by Eq. (4.48). For this choice, the integration in Eq. (4.30) yields

$$G_{\pm}(y) = \mp\frac{2\sigma y \pm V \log\left|1 + e^{2\sigma y} \pm V\right|}{2\sigma(1 \pm V)}. \tag{4.66}$$

As was the case in Chapter 3, we have to make a case distinction due to the $|1+e^{2z^1\sigma} - V|$ term:

$$|1 + e^{2y\sigma} - V| = \begin{cases} 1 + e^{2y\sigma} - V, & V < 1 + e^{2y\sigma} \\ -(1 + e^{2y\sigma} - V), & V > 1 + e^{2y\sigma} \end{cases} \tag{4.67}$$

The solution is well-defined for the case of $V < 1$ because then $|1+e^{2z^1\sigma} - V| = 1+e^{2z^1\sigma} - V$ and the inverse of $G_-(y)$ is well-defined. If $V > 1$, $G_-(y)$ has a singularity and the case distinction has to be taken into account. Ultimately, with this method we can only analyze $V < 1$ cases.

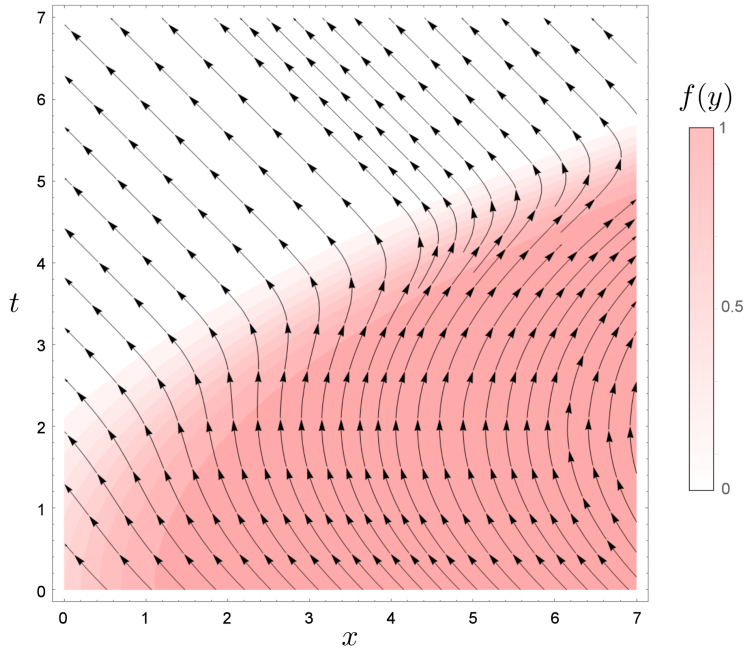

Figure 4.4: A spacetime diagram of left-moving (x_+) light rays for the Alcubierre metric. The same parameters are taken as in Fig. 4.3.

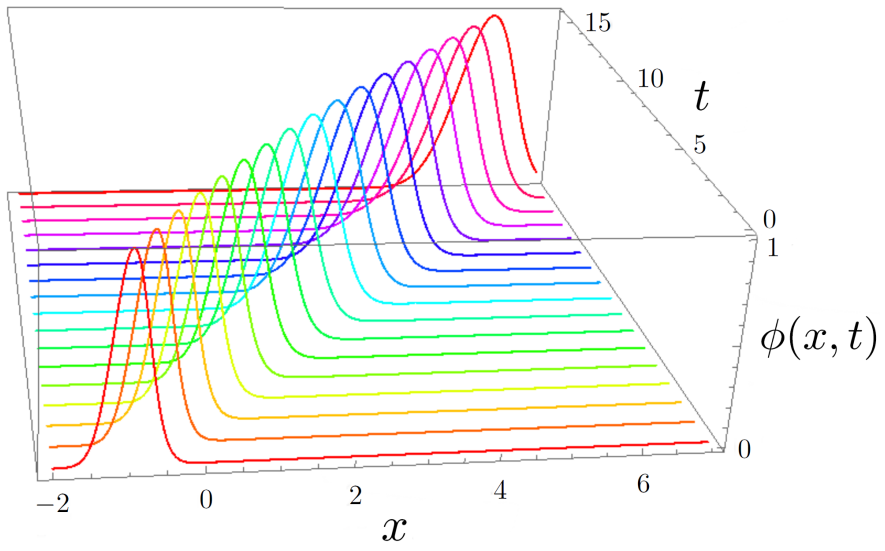

Figure 4.5: A wavepacket expands upon entering a $V = 0.6$, $\sigma = 1$ warp drive. This result comes from using the solution to the wave equation in conformal light-cone coordinates (Eq. (4.42)) with the shaping function of Eq. (4.48). This result is identical to the results obtained using conformal coordinate transformations in Section 3.4.

We will conclude by examining the relationship between x-t coordinates and light-cone coordinates for an accelerating warp drive. For a curved two-dimensional spacetime, we can generally express a set of light-cone coordinates in the form $x_\pm = \frac{1}{\sqrt{2}}(X \pm T)$. Explicitly, the light-cone coordinates of Eq. (4.59) look like

$$x_+ = -\frac{\log\left(\sqrt{\pi}e^{\frac{\sigma}{a}}\sqrt{\frac{\sigma}{a}}\left(\operatorname{erf}\left(\sqrt{\frac{\sigma}{a}}\right) - \operatorname{erf}\left(\sqrt{\frac{\sigma}{a}}(at+1)\right)\right) + \left(e^{-2\sigma y}-1\right)e^{-\sigma-t(at+2)} + 1\right)}{2\sqrt{2}\sigma} \tag{4.68}$$

$$x_- = -\frac{\log\left(\sqrt{\pi}e^{\frac{\sigma}{a}}\sqrt{\frac{\sigma}{a}}\left(\operatorname{erf}\left(\sqrt{\frac{\sigma}{a}}\right) - \operatorname{erf}\left(\sqrt{\frac{\sigma}{a}}(1-at)\right)\right) + \left(e^{-2\sigma y}-1\right)e^{\sigma t(2-at)} + 1\right)}{2\sqrt{2}\sigma} \tag{4.69}$$

Solving for the functional forms of X and T, we find

$$\begin{aligned} X = &-\frac{1}{4\sigma}\log\left(1 + e^{t(2-at)\sigma}u + e^{\sigma/a}\sqrt{\pi}\sqrt{\frac{\sigma}{a}}\left(\operatorname{erf}\left(\sqrt{\frac{\sigma}{a}}\right) - \operatorname{erf}\left((1-at)\sqrt{\frac{\sigma}{a}}\right)\right)\right) \\ &-\frac{1}{4\sigma}\log\left(1 + e^{-t(2+at)\sigma}u + e^{\sigma/a}\sqrt{\pi}\sqrt{\frac{\sigma}{a}}\left(\operatorname{erf}\left(\sqrt{\frac{\sigma}{a}}\right) - \operatorname{erf}\left((1+at)\sqrt{\frac{\sigma}{a}}\right)\right)\right) \end{aligned} \tag{4.70}$$

$$\begin{aligned} T = &\frac{1}{4\sigma}\log\left(\sqrt{\pi}e^{\frac{\sigma}{a}}\sqrt{\frac{\sigma}{a}}\left(\operatorname{erf}\left(\sqrt{\frac{\sigma}{a}}\right) - \operatorname{erf}\left(\sqrt{\frac{\sigma}{a}}(1-at)\right)\right) + u\,e^{\sigma t(2-at)} + 1\right) \\ &-\frac{1}{4\sigma}\log\left(\sqrt{\pi}e^{\frac{\sigma}{a}}\sqrt{\frac{\sigma}{a}}\left(\operatorname{erf}\left(\sqrt{\frac{\sigma}{a}}\right) - \operatorname{erf}\left(\sqrt{\frac{\sigma}{a}}(at+1)\right)\right) + u\,e^{\sigma(-t)(at+2)} + 1\right) \end{aligned} \tag{4.71}$$

where $u = \left(-1 + e^{-2y\sigma}\right)$. Making the substitution $y = x - x_{\rm o}(t)$ will give us $T(x,t)$ and $X(x,t)$. To get an idea of how these functions depend on x and t, we can plot the contour lines. These are shown in Fig. 4.6 and Fig. 4.7.

It should be possible to develop animations (as we did in Section 3.4) for the propagation of waves in an accelerating warp drive. This may yield new insights into the behaviour of light in the Alcubierre spacetime. However, this is left for future work. The developments in this chapter are recent and so a full analysis is not presented here. Further remarks about future work will be discussed in the concluding chapter.

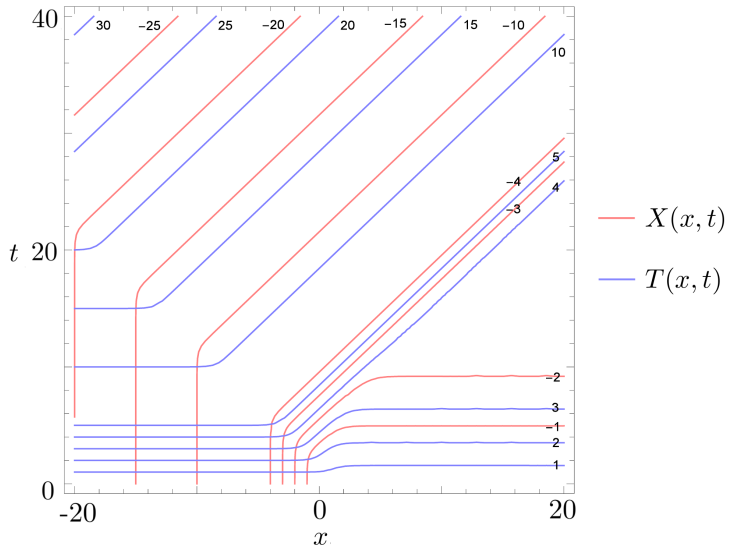

Figure 4.6: Lines of constant $X(x,t)$ and $T(x,t)$ for a linearly accelerating warp drive. The parameters are $x_o(t) = \frac{1}{2}at^2$ with $a = 0.1$, $\sigma = 1$. The red lines represent constant X from Eq. (4.70) and the blue lines represent constant T from Eq. (4.71).

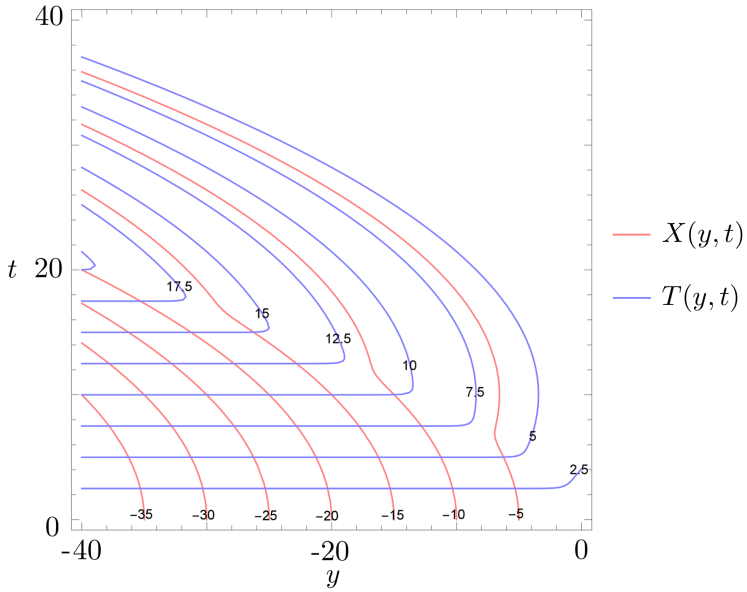

Figure 4.7: Lines of constant $X(y,t)$ and $T(y,t)$ for a linearly accelerating warp drive. The horizontal axis is $y = x - x_o(t)$. The parameters are the same as in Fig. 4.6 with the red lines representing constant X and the blue lines representing constant T.

Chapter 5

Conclusion

5.1 Summary

Within the context of general relativity, the Alcubierre metric allows for apparent faster-than-light travel. An object in this spacetime could achieve arbitrarily large velocities without experiencing any time dilation or tidal forces. This parallels the "warp drive" of science fiction literature and film. Although the construction of a warp drive is beyond the current reach of humanity, it is still useful and interesting to study the Alcubierre metric. First, it could reveal potential "technosignatures" of a warp drive in the cosmos. If another intelligent civilization has constructed one, it may be possible to detect its presence if we know what to look for. Second, the Alcubierre metric provides a unique opportunity to study time-dependent horizons. There are only a small number of solutions in general relativity that have this property [22] and so the Alcubierre metric could provide new insights into horizon formation. Finally, this spacetime is a fascinating object to study: it is the mathematical analog of a phenomenal and futuristic technology. That's enough to capture my curiosity and interest.

To date, only a handful of papers have examined the problem of light propagation in the Alcubierre metric. These studies have been restricted to numerical techniques and so an analytic description was lacking in the literature. This thesis fills that gap by presenting an analytic description of light propagation in the Alcubierre metric.

In Chapter 2, the wave equation for the Alcubierre metric was calculated from the metric tensor. The wave equation is difficult to solve analytically in the original x-t coordinate system and so a novel approach was developed based on conformal coordinate transformations. In Chapter 3, a coordinate transformation was found that reduces the Alcubierre metric to the conformally flat metric. This permits us to solve the wave equation for the case of $V = \text{constant}$, $V < 1$. It is found that wavepackets traveling into a warp drive undergo an apparent expansion or contraction. This corresponds to an apparent redshift or blueshift from the perspective of an outside observer at rest. This result is found to agree numerically with predictions by Clark et. al [23]. For the case of $V > 1$, the coordinate transformation is discontinuous which presents obstacles to describing light propagation in faster-than-light warp drives. In Chapter 4, a method based on light-cone coordinates was developed. This permits us to analyze $V > 1$ warp drives and accelerating warp drives. It also allows us to analyze the formation of the apparent horizon.

5.2 Future Work

The work of Chapter 4 is recent and so there is still much to explore. For instance, it would be worthwhile to construct visuals of how a wavepacket would transform as it passes through the boundary of an accelerating warp drive. What would happen to a wavepacket that is "straddling" the boundary of the warp bubble when it goes from $V < 1$ to $V > 1$? Would it get ripped apart? What would happen to light that is sent forward from the inside of a $V > 1$ warp drive? Would it "get stuck" at the front boundary of the warp bubble? Many interesting questions remain!

It would also be worthwhile to investigate a numerical solution to the wave equation (Eq. (2.21)). This would provide a sanity check for the results of Chapter 3. It may also permit us to consider other scenarios (for instance, a warp drive in three spatial dimensions) that were not investigated in this thesis.

Another avenue of future work is quantum field theory in curved space. It has been predicted that the formation of a horizon will result in the emission of radiation [20] [37] . One notable example is *Hawking radiation*: quantum effects near the event horizon of a black hole will result in the emission of particles [38]. Another example is the *Unruh effect* where an accelerating observer will observe blackbody radiation due to the formation of an apparent horizon [39]. Since an apparent horizon forms for a $V > 1$ warp drive, there may be an effect similar to Hawking radiation or Unruh radiation. Some preliminary work on this question has been performed by Hiscock [35]. However, there is still much that can be done. Now that we've developed a description of an accelerating warp drive, this is one interesting question for future study.

Bibliography

[1] J. Hartle, *Gravity : An Introduction to Einstein's General Relativity*, Addison-Wesley, San Francisco, USA, first edition, 2003.

[2] A. DeBenedictis, The physics and mathematics of warp drive, webpage, http://www.sfu.ca/~adebened/funstuff/warpdrive.html, accessed 2017-03-09.

[3] Y. Fujii and K. Maeda, *The Scalar-Tensor Theory of Gravitation*, Cambridge University Press, Cambridge, UK, first edition, 2002.

[4] B. Zwiebach, *A First Course in String Theory*, Cambridge University Press, Cambridge, UK, second edition, 2004.

[5] C. M. Will, Living Rev. Relativ. **9**, 3 (2006).

[6] R. V. Pound and G. A. Rebka, Phys. Rev. Lett. **3**, 439 (1959).

[7] B. Abbott et al., Phys. Rev. Lett. **116**, 241103 (2016).

[8] M. Alcubierre, Class. Quantum Grav. **11**, L73 (1994).

[9] M. J. Pfenning and L. H. Ford, Class. Quantum Grav. **14**, 1743 (1997).

[10] F. S. N. Lobo and M. Visser, Class. Quantum Grav. **21**, 5871 (2004).

[11] D. H. Coule, Class. Quantum Grav. **15**, 2523 (1998).

[12] S. K. Lamoreaux, Phys. Rev. Lett. **78**, 5 (1997).

[13] G. Bressi, G. Carugno, R. Onofrio, and G. Ruoso, Phys. Rev. Lett. **88**, 041804 (2002).

[14] C. V. D. Broeck, Class. Quantum Grav. **16**, 3973 (1999).

[15] F. J. Dyson, Science **131**, 1667 (1960).

[16] C. Sagan and R. G. Walker, Astrophys. J. **144**, 1216 (1966).

[17] M. J. Harris, J. Br. Interplanet. Soc. **55**, 383 (2002).

[18] J. N. Benford and D. J. Benford, Astrophys. J. **825**, 101 (2016).

[19] M. Lingam and A. Loeb, Astrophys. J. **837**, L23 (2017).

[20] L. C. B. Crispino, A. Higuchi, and G. E. A. Matsas, Rev. Mod. Phys. **80**, 787 (2008).

[21] W. Rindler, Mon. Not. R. Astron. Soc. **116**, 662 (1956).

[22] V. Faraoni, Galaxies **1**, 114 (2013).

[23] C. Clark, W. A. Hiscock, and S. L. Larson, Class. Quantum Grav. **16**, 3965 (1999).

[24] T. Müller and D. Weiskopf, Gen. Relativ. Gravitation **44**, 509 (2011).

[25] D. Weiskopf, in *Proceedings of the Conference on Visualization*, pages 445–448, Los Alamitos, USA, 2000, IEEE Computer Society Press.

[26] T. H. Anderson, T. G. Mackay, and A. Lakhtakia, J. Opt. **13**, 055107 (2011).

[27] U. Leonhardt and P. Piwnicki, Phys. Rev. A **60**, 4301 (1999).

[28] A. M. Volkov, A. A. Izmestev, and G. V. Skrotskii, J. Exp. Theor. Phys. **32**, 686 (1971).

[29] A. Everett and T. Roman, *Time Travel and Warp Drives: A Scientific Guide to Shortcuts Through Time and Space*, University of Chicago Press, Chicago, USA, first edition, 2011.

[30] S. V. Krasnikov, Phys. Rev. D **57**, 4760 (1998).

[31] K. D. Olum, Phys. Rev. Lett. **81**, 3567 (1998).

[32] R. J. Low, Class. Quantum Grav. **16**, 543 (1999).

[33] L. D. Landau and E. Lifshitz, *The Classical Theory of Fields*, Pergamon Press, Oxford, UK, fourth edition, 1980.

[34] A. Steane, *Relativity Made Relatively Easy*, OUP Oxford, Oxford, UK, first edition, 2012.

[35] W. A. Hiscock, Class. Quantum Grav. **14**, L183 (1997).

[36] P. V. O'Neil, *Beginning Partial Differential Equations*, Wiley, Hoboken, USA, third edition, 2014.

[37] S. Hawking, Nature **248**, 30 (1974).

[38] D. N. Page, Phys. Rev. D **13**, 198 (1976).

[39] W. G. Unruh, Phys. Rev. D **14**, 870 (1976).

[40] T. Padmanabhan, *Gravitation: Foundations and Frontiers*, Cambridge University Press, Cambridge, UK, first edition, 2010.

Appendix A

Christoffel Symbols for the Alcubierre Metric

The Christoffel symbols are a tensor-like object that can be used to describe the geometry of the metric. In most cases, the Christoffel symbols can be computed by finding the equations of motion for geodesics and reading off the Christoffel symbols from them. In practice, it is much more convenient to use a computer to quickly perform the calculations. We use the GREAT.M package in Mathematica. The following notation is used below:

$$
\begin{aligned}
f &\equiv f(x^0, x^1, x^2, x^3) & V &\equiv V(x^0) \\
k &\equiv 1 + f(x^0, x^1, x^2, x^3)^2\, V(x^0)^2 & \partial_\alpha &\equiv \frac{\partial}{\partial x^\alpha} \\
h &\equiv f(x^0, x^1, x^2, x^3)^2\, V(x^0)^2 - 1
\end{aligned}
$$

The Alcubierre metric is given by Eq. (2.6). Christoffel symbols for the Alcubierre metric are

$$
\Gamma^0_{\alpha\beta} = \begin{pmatrix}
f^2 V^3 (\partial_1 f) & -f V^2 (\partial_1 f) & -\frac{1}{2} f V^2 (\partial_2 f) & -\frac{1}{2} f V^2 (\partial_3 f) \\
-f V^2 (\partial_1 f) & V (\partial_1 f) & V (\partial_2 f)/2 & V (\partial_3 f)/2 \\
-\frac{1}{2} f V^2 (\partial_2 f) & V (\partial_2 f)/2 & 0 & 0 \\
-\frac{1}{2} f V^2 (\partial_3 f) & V (\partial_3 f)/2 & 0 & 0
\end{pmatrix}
$$

$$
\Gamma^1_{\alpha\beta} = \begin{pmatrix}
f \left(h V^2 (\partial_1 f) - V'\right) - V (\partial_0 f) & -f^2 V^3 (\partial_1 f) & -k V (\partial_2 f)/2 & -k V (\partial_3 f)/2 \\
-f^2 V^3 (\partial_1 f) & f V^2 (\partial_1 f) & f V^2 (\partial_2 f)/2 & f V^2 (\partial_3 f)/2 \\
-k V (\partial_2 f)/2 & f V^2 (\partial_2 f)/2 & 0 & 0 \\
-k V (\partial_3 f)/2 & f V^2 (\partial_3 f)/2 & 0 & 0
\end{pmatrix}
$$

$$
\Gamma^2_{\alpha\beta} = \begin{pmatrix}
-f V^2 (\partial_2 f) & V (\partial_2 f)/2 & 0 & 0 \\
V (\partial_2 f)/2 & 0 & 0 & 0 \\
0 & 0 & 0 & 0 \\
0 & 0 & 0 & 0
\end{pmatrix}
\qquad
\Gamma^3_{\alpha\beta} = \begin{pmatrix}
-f V^2 (\partial_3 f) & V (\partial_3 f)/2 & 0 & 0 \\
V (\partial_3 f)/2 & 0 & 0 & 0 \\
0 & 0 & 0 & 0 \\
0 & 0 & 0 & 0
\end{pmatrix}
$$

The lower two indices of $\Gamma^\alpha_{\beta\gamma}$ are symmetric. The upper index α corresponds to the equation of motion for the x^α coordinate (Eq. (1.20)).

Appendix B

Null Geodesics & The Eikonal Equation

Several papers have already calculated the trajectories of light rays in the Alcubierre metric [23] [24] [26]. Although a study of null geodesics is not presented in this thesis, it is still useful to have an understanding for how these earlier results were obtained.

We have already established that particle dynamics will obey Eq. (1.18) and that their freely-falling trajectories will be described by Eq. (1.20). Now we must modify this description for photons which have zero rest mass. These particles move along *null worldlines* which are lines for which $ds^2 = 0$. In this situation, the proper time τ is no longer a valid parameter to characterize their trajectories. This is because the proper time is unchanging along a null worldline. As such, a new parameter must be chosen.

Null worldlines are generally written in terms of the *four-velocity vector* u^α. The four-velocity is defined as

$$u^\alpha = \frac{dx^\alpha}{d\lambda}. \tag{B.1}$$

The four-velocity has components that are the derivatives of position everywhere along the particle's worldline. It also has the property that

$$g_{\alpha\beta}\, u^\alpha\, u^\beta = 0. \tag{B.2}$$

This means that the four-velocity is everywhere tangent to the worldline. With such a parametrization by λ, the equation of motion for a light ray is equivalent to

$$\frac{du^\alpha}{d\lambda} = 0. \tag{B.3}$$

In this context, we can define a geodesic equation similar to Eq. (1.20) for particles traveling along null worldlines. This equation is known as the *null geodesic equation* and is given by

$$\frac{d^2x^\alpha}{d\lambda^2} = -\Gamma^\alpha_{\beta\gamma}\frac{d^2x^\beta}{d\lambda^2}\frac{d^2x^\gamma}{d\lambda^2}. \tag{B.4}$$

Curves satisfying Eq. (B.4) are called *null geodesics*.

The trajectory of a photon can also be calculated from the Eikonal approximation. In the

Eikonal approximation, it is assumed that the wavelength of light approaches 0. The ansatz is then made that the electric field takes the form of a wave with a slowly varying phase,

$$E(\vec{r}) = A(\vec{r})\, e^{ikS(\vec{r})}, \tag{B.5}$$

so that the rays travel through surfaces of constant phase. The Eikonal equation in a curved spacetime for a field ψ can be found to be

$$g^{\alpha\beta}\, \partial_\beta\psi\, \partial_\alpha\psi \;=\; 0. \tag{B.6}$$

We will derive this using the methods of perturbation theory. The derivation begins with the wave equation for a scalar field ϕ.

$$g^{\alpha\beta}\nabla_\alpha\nabla_\beta\phi = 0 \tag{B.7}$$

A small perturbation ϵ is applied.

$$\phi = (a + \epsilon b + ...)\, e^{i\psi/\epsilon} \tag{B.8}$$

The first derivative in the wave equation then takes the form

$$\begin{aligned} \nabla_\beta\phi &= \nabla_\beta(a + \epsilon b + ...)\, e^{i\psi/\epsilon} + \nabla_\beta\, e^{i\psi/\epsilon}\, (a + \epsilon b + ...) \\ &= \nabla_\beta(a + \epsilon b + ...)\, e^{i\psi/\epsilon} + i/\epsilon\nabla_\beta\psi\, e^{i\psi/\epsilon}(a + \epsilon b + ...). \end{aligned} \tag{B.9}$$

Upon performing the product rule,

$$\begin{aligned} \nabla_\alpha\nabla_\beta\phi \;=& (a + \epsilon b + ...)\, (i^2/\epsilon^2\, \nabla_\beta\psi\, \nabla_\alpha\psi\, e^{i\psi/\epsilon} + (i/\epsilon)\, e^{i\psi/\epsilon}\, \nabla_\alpha\nabla_\beta\psi) \\ &+ \nabla_\beta(a + \epsilon b + ...)(i/\epsilon)\, \nabla_\alpha\psi\, e^{i\psi/\epsilon} \\ &+ i/\epsilon\, \nabla_\beta\psi\, e^{i\psi/\epsilon}\, \nabla_\alpha(a + \epsilon b + ...) \\ &+ \nabla_\alpha\nabla_\beta(a + \epsilon b + ...)\, e^{i\psi/\epsilon} = 0. \end{aligned} \tag{B.10}$$

To simplify, we let $\Omega = (a + \epsilon b + ...)$. The equation is rewritten

$$\begin{aligned} \nabla_\alpha\nabla_\beta\, \phi \;=\; & i/\epsilon\, \nabla_\beta\Omega\, \nabla_\alpha\psi\, e^{i\psi/\epsilon} \;+\; \nabla_\alpha\nabla_\beta\, \Omega\, e^{i\psi/\epsilon} \\ & +\; \Omega\, e^{i\psi/\epsilon}(-1/\epsilon^2\, (\nabla_\beta\psi\, \nabla_\alpha\psi) \;+\; i/\epsilon\, \nabla_\alpha\nabla_\beta\psi)\,) \\ & +\; i/\epsilon\, \nabla_\alpha\Omega\, (\nabla_\beta\, \psi)\, e^{i\psi/\epsilon} \\ =\; & e^{i\psi/\epsilon}\, \Big(i/\epsilon\, (\nabla_\beta\Omega)\, (\nabla_\alpha\psi) \\ & +\; (\nabla_\alpha\nabla_\beta\Omega) \;+\; \Omega\, (-1/\epsilon^2\, (\nabla_\beta\psi)(\nabla_\alpha\psi)\,) \\ & +\, \Omega\, (i/\epsilon)\, (\nabla_\alpha\nabla_\beta\psi) \;+\; i/\epsilon\, (\nabla_\alpha\Omega)\, (\nabla_\beta\psi)\, \Big) = 0. \end{aligned} \tag{B.11}$$

By definition, $\nabla_\gamma \psi = k_\gamma$. This simplifies things to

$$\begin{aligned}\nabla_\alpha \nabla_\beta \, \phi = e^{i\psi/\epsilon} \Big(i/\epsilon \, (\nabla_\beta \Omega) \, k_\alpha \; + \; (\nabla_\alpha \nabla_\beta \Omega) \; + \; \Omega(-1/\epsilon^2 \, k_\beta \, k_\alpha \,) + \\ \Omega \, (i/\epsilon) \, (\nabla_\alpha k_\beta) \; + \; i/\epsilon \, (\nabla_\alpha \Omega) \, k_\beta \Big) = 0.\end{aligned} \tag{B.12}$$

To leading order in ϵ, this yields

$$0 \; = \; e^{i\psi/\epsilon}(a + \epsilon b + ...) \, (-1/\epsilon^2) \, (k_\beta k_\alpha) \tag{B.13}$$

which implies $k_\beta k_\alpha = 0$. Now multiplying by the inverse metric $g^{\alpha\beta}$ yields

$$k^\alpha k_\alpha = 0 \tag{B.14}$$

or

$$g^{\alpha\beta} \, \partial_\beta \psi \, \partial_\alpha \psi \; = \; 0 \tag{B.15}$$

which is the Eikonal equation.

The null geodesic equation can be derived from Eq. (B.15). To do so, we take the derivative of both sides of Eq. (B.14),

$$0 = \nabla_\beta (k^\alpha k_\alpha). \tag{B.16}$$

To simplify, we write the wave four-vector as the derivative of a scalar function so that $k^\alpha = \nabla^\alpha \psi$ and $k_\alpha = \nabla_\alpha \psi$. In this form, Eq. (B.14) becomes

$$0 = \nabla_\alpha \psi \nabla_\beta \nabla^\alpha \psi \; + \; \nabla^\alpha \psi \nabla_\beta \nabla_\alpha \psi \tag{B.17}$$

by the product rule. This equation can be simplified by using the raising and lowering properties of the metric tensor: $\nabla^\alpha (g_{\alpha\beta} \, \psi) = \nabla_\beta (\psi)$ and $\nabla^\alpha (\psi) = \nabla_\beta (g^{\beta\alpha} \, \psi)$. Then

$$\nabla^\alpha \psi = \nabla_\gamma g^{\gamma\alpha} \psi \tag{B.18}$$

and by exploiting the property that $\nabla_\gamma g^{\gamma\alpha} = 0$, we can write

$$\nabla^\alpha \psi = \nabla_\gamma g^{\gamma\alpha} \psi = g^{\gamma\alpha} \nabla_\gamma \psi. \tag{B.19}$$

In other words, the metric can be factored out of the covariant derivative. This permits us to write

$$\nabla_\beta g^{\gamma\alpha} \nabla_\gamma \psi = g^{\gamma\alpha} (\nabla_\beta \nabla_\gamma \psi) \tag{B.20}$$

and Eq. (B.17) takes the form

$$\begin{aligned} 0 &= (\nabla_\alpha g^{\gamma\alpha}\psi)(\nabla_\beta\nabla_\gamma\psi) + (\nabla^\alpha\psi\nabla_\beta\nabla_\alpha\psi) \\ &= (\nabla^\gamma\psi)(\nabla_\beta\nabla_\gamma\psi) + (\nabla^\alpha\psi\nabla_\beta\nabla_\alpha\psi). \end{aligned} \tag{B.21}$$

The γ indices can be arbitrarily relabeled without loss of generality. Upon doing so, the equation becomes

$$0 = 2\,(\nabla^\alpha\psi\nabla_\beta\nabla_\alpha\psi). \tag{B.22}$$

By commutivity of scalar derivatives,

$$\begin{aligned} 0 =& 2\,(\nabla^\alpha\psi\nabla_\alpha\nabla_\beta\psi) \\ &= 2\,k^\alpha\nabla_\alpha k_\beta \\ &= k^\alpha\nabla_\alpha k_\beta \end{aligned} \tag{B.23}$$

This is simply the null geodesic equation written in a disguised form. Writing the covariant derivative out in all its glory, Eq. (B.23) becomes

$$\begin{aligned} 0 &= k^\alpha\left(\frac{\partial k_\beta}{\partial x^\alpha} - \Gamma^\delta_{\beta\gamma}k_\delta\right) \\ &= k^\alpha\,\frac{\partial k_\beta}{\partial x^\alpha} - \Gamma^\delta_{\beta\gamma}k_\delta k^\alpha. \end{aligned} \tag{B.24}$$

So how is this related to the standard null geodesic equation? If we parametrize the curve (the geodesic) as $x^\mu(s)$, then the tangent vector is $T^\mu = \frac{dx^\mu}{ds}$. This means $T^\alpha\partial_\alpha = \frac{d}{ds}$. Finally, we get

$$\frac{d}{ds}\frac{dx^\beta}{ds} + \Gamma^\beta_{\alpha\gamma}\frac{dx^\alpha}{ds}\frac{dx^\gamma}{ds} = 0 \tag{B.25}$$

which is precisely the null geodesic equation. For further reading, a good treatment of the subject is given in [40].